



Fermi National Accelerator Laboratory

FERMILAB-TM-2090

Intensity Dependent Instability Issues for Electron Rings

K.Y. Ng

*Fermi National Accelerator Laboratory
P.O. Box 500, Batavia, Illinois 60510*

September 1999

Disclaimer

This report was prepared as an account of work sponsored by an agency of the United States Government. Neither the United States Government nor any agency thereof, nor any of their employees, makes any warranty, expressed or implied, or assumes any legal liability or responsibility for the accuracy, completeness, or usefulness of any information, apparatus, product, or process disclosed, or represents that its use would not infringe privately owned rights. Reference herein to any specific commercial product, process, or service by trade name, trademark, manufacturer, or otherwise, does not necessarily constitute or imply its endorsement, recommendation, or favoring by the United States Government or any agency thereof. The views and opinions of authors expressed herein do not necessarily state or reflect those of the United States Government or any agency thereof.

Distribution

Approved for public release; further dissemination unlimited.

Copyright Notification

This manuscript has been authored by Universities Research Association, Inc. under contract No. DE-AC02-76CH03000 with the U.S. Department of Energy. The United States Government and the publisher, by accepting the article for publication, acknowledges that the United States Government retains a nonexclusive, paid-up, irrevocable, worldwide license to publish or reproduce the published form of this manuscript, or allow others to do so, for United States Government Purposes.

DRAFT

TM-2090

INTENSITY DEPENDENT INSTABILITY ISSUES FOR ELECTRON
RINGS

King-Yuen Ng

Fermi National Accelerator Laboratory, P.O. Box 500, Batavia, IL 60510*

(August 2-6, 1999)

LNLS, Campinas

*Operated by the Universities Research Association, Inc., under contract with the U.S. Department of Energy.

CONTENTS

- 1 Longitudinal focusing
- 2 Longitudinal microwave instability
 - 2.1 Mode-mixing instability
 - 2.2 Bunch lengthening and scaling law
 - 2.3 Sawtooth instability
- 3 Robinson instability
- 4 Longitudinal coupled-bunch instability
 - 4.1 Coupled modes and growth rates
 - 4.2 Higher-harmonic cavities
 - 4.3 Rf voltage modulation
- 5 Transverse focusing and transverse wake
- 6 Transverse collective instabilities
 - 6.1 Separation of transverse and longitudinal motions
 - 6.2 Chromaticity frequency shift
- 7 Transverse coupled-bunch instabilities
 - 7.1 Resistive wall
 - 7.2 Narrow resonances
- 8 Head-tail instabilities
- 9 Strong head-tail instability
- References

1 LONGITUDINAL FOCUSING

A bunch of electrons has a spread of energy because of many reasons, for example, random quantum excitation which changes the energy of the particles randomly, intrabeam scattering which is just Coulomb scattering among the particles, and Touschek scattering [1] which is large-angle Coulomb scattering which converts the transverse momentum of a particle into longitudinal. In an accelerator ring or storage ring, particles with different energies have different closed orbits, their lengths are given by

$$C = C_0 [1 + \alpha_0 \delta + \mathcal{O}(\delta^2)] , \quad (1.1)$$

where δ is the fractional spread in momentum and C_0 is the orbit length of the so-called *on-momentum* particle. The proportionality constant α_0 is called the momentum-compaction factor of the accelerator ring. Here, we assume the velocity of the on-momentum electron to be c , the velocity of light; therefore fraction momentum spread $\delta = \Delta p/p_0$ will be the same as fraction energy spread $\Delta E/E_0$, where p_0 and E_0 are the momentum and energy of the on-momentum particle. For most electron rings, $\alpha_0 > 0$, implying that particles with larger energy will travel along a longer closed orbit. Thus the period of revolution will be relatively longer. Therefore, particles with lower energies will slip ahead by ΔT every turn, while particle with higher energies will slip behind. The particles will spread out longitudinally and the bunch will be destroyed. The *slip factor* η is defined as

$$\eta = \frac{\Delta T}{T_0} = \frac{\Delta C}{C_0} - \frac{\Delta v}{v_0} = \alpha_0 - \frac{1}{\gamma^2} , \quad (1.2)$$

where T_0 and v_0 are, respectively, the revolution period and velocity of the on-momentum particle, and $\gamma = E_0/m_e$, m_e being the electron rest mass. With $v_0 = c$, we have actually $\eta = \alpha_0$ and we called the operation *above the transition energy*. For low-energy hadron rings, the velocity term may dominate making $\eta < 0$ and we say the operation is *below the transition energy*. Obvious the transition energy is defined as $E_t = \gamma_t m_0 c^2$, where m_0 is the rest mass of the particle and $\gamma_t = \alpha_0^{-1/2}$.

In order to have the particle bunched, a longitudinal focusing force will be required. This is done by the introduction of rf cavities. Consider 3 particles arriving in the first turn at exactly same time at a cavity gap, where the rf sinusoidal voltage curve is at 180° , as shown in Fig. 1a. All three particles are not gaining any energy from the rf wave. One turn later, the on-momentum particle arrives at the cavity gap at exactly the time when the rf sinusoidal voltage curve is again at 180° and gains no energy. The lower energy particle arrives at the gap earlier by τ_1 , which we call *time slip*. It sees the positive part of the rf voltage and gains energy, as illustrated in Fig. 1b. For the second turn, it will arrive at the gap earlier by $\tau_1 + \tau_2$, where $\tau_2 < \tau_1$ because the particle energy have been raised in the second passage. This particle will continue to gain energy from the rf every turn and its turn-by-turn additional time slip diminishes. Eventually, this particle will have an energy higher than the on-momentum particle and starts to arrive at the cavity gap later turn after turn, or its turn-by-turn time slip becomes negative. Similar conclusion can be drawn for the particle that has energy initial energy higher than the on-momentum particle. With the rf voltage wave, the off-momentum particles will oscillates around the on-momentum particle and continue to form a bunch. In reality, the particles lose an amount of energy U_s every turn due to synchrotron radiation. This is compensated by shifting the rf phase slightly from 180° to $\phi_s = \sin^{-1}(U_s/V_{\text{rf}})$ so that the on-momentum electron will see the rf voltage at the phase ϕ_s when traversing the cavity gap. This particle is also called

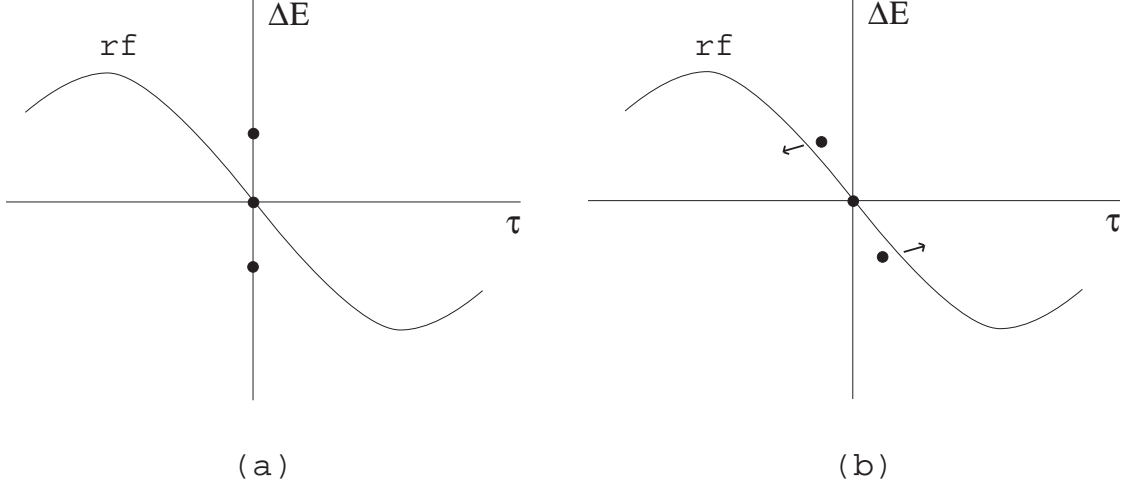


Figure 1: Three particles are shown in the longitudinal phase planes. (a) Initially, there are all at the rf phase of 180° and do not gain or lose any energy. (b) One turn later, the on-momentum particle arrives with the same phase of 180° without any change in energy. The particle with lower energy arrives earlier and gains energy from the positive part of the rf at phase $< 180^\circ$. The particle with higher energy arrives late and loses energy because it sees the rf at phase $> 180^\circ$.

the *synchronous* particle. The equations of motion can be written as

$$\frac{d\tau}{dn} = -\alpha_0 T_0 \frac{\Delta E}{E_0}, \quad (1.3)$$

$$\frac{d\Delta E}{dn} = eV_{\text{rf}}[\sin(\phi_s - h\omega_0\tau) - \sin\phi_s] - [U(\delta) - U_s], \quad (1.4)$$

where $\omega_0/(2\pi) = 1/T_0$ is the revolution frequency of the ring, V_{rf} is the rf voltage (the peak value of the rf wave), and h is the rf harmonic, which is the number oscillations the rf wave makes during one revolution period. Here e is the absolute value of the electron charge. We neglect the small difference between the energy lost $U(\delta)$ by the off-momentum particle and the energy lost U_s by the on-momentum particle. For small amplitude oscillations, the above can be simplified to

$$\frac{d^2\tau}{dn^2} - \frac{2\pi\alpha_0 h e V_{\text{rf}} \cos\phi_s}{E_0} \tau = 0. \quad (1.5)$$

Therefore, the bunch particles are oscillating with a tune

$$\nu_s = \sqrt{-\frac{\alpha_0 h e V_{\text{rf}} \cos\phi_s}{2\pi E_0}}, \quad (1.6)$$

which we called the *synchrotron tune*, from which we obtain the synchrotron frequency $\omega_s/(2\pi) = \nu_s \omega_0/(2\pi)$. The negative sign inside the square root implies that ϕ_s should be near 180° in the second quadrant. When the oscillation amplitude is larger, the sine wave cannot be linearized. The focusing force is smaller and the synchrotron tune will become smaller. In other words, there will be a spread in the synchrotron tune which will be very essential to the Landau damping of the collective instabilities to be discussed later. As the

oscillation amplitude continue to increase, a point will be reached when there is no more focusing provided anymore. This boundary in the τ - ΔE phase space gives the maximum possible bunch area allowed and is called the *bucket* holding the bunch. Any particle that goes outside the bucket will be lost.

2 LONGITUDINAL MICROWAVE INSTABILITY

The beam particles interact with the discontinuities of the vacuum chamber leaving an electromagnetic *wake* which acts on the particles behind and disturbs their motion. Under some conditions, this disturbance will accumulate leading to the growths of the bunch length, transverse sizes, momentum spread, etc. The effects can be so violent that some parts of the beam or the whole beam may be lost. These are called collective instabilities, because some particular collective modes of oscillation inside the bunch are excited. We will start in this section the study of the longitudinal microwave instability driven by a short longitudinal wake.

The equations of motion of Eqs. (1.3) and (1.4) are now replaced by

$$\frac{d\tau}{dn} = -\alpha_0 T_0 \frac{\Delta E}{E_0}, \quad (2.1)$$

$$\frac{d\Delta E}{dn} = eV_{\text{rf}}[\sin(\phi_0 - h\omega_0\tau) - \sin\phi_0] - [U(\delta) - U_0] + C_0(\langle F_0^{\parallel} \rangle - \langle F_{0s}^{\parallel} \rangle), \quad (2.2)$$

where the additional term, $C_0\langle F_0^{\parallel} \rangle$, is the energy gained by the particle in a turn due to the average electromagnetic wake potential left by the preceding particles. It can be expressed as

$$C_0\langle F_0^{\parallel}(\tau) \rangle = e^2 \int_{\tau}^{\infty} d\tau' \rho(\tau') W_0'(\tau' - \tau), \quad (2.3)$$

where $W_0'(\tau)$ is the monopole longitudinal *wake function*, or the integrated energy received by a witness particle of unit charge from a source particle of unit charge that has a relative time advance τ . The wake potential is casual, meaning that $W_0'(\tau) = 0$ when $\tau < 0$. This is the description in the time domain. In the frequency domain, we talk about the monopole *longitudinal impedance*, $Z_0^{\parallel}(\omega)$, of the vacuum chamber, which is defined as Fourier transform of the longitudinal wake function:

$$Z_0^{\parallel}(\omega) = \int_{-\infty}^{\infty} e^{i\omega\tau} W_0'(\tau) d\tau. \quad (2.4)$$

It has the same dimension as the impedance in a circuit. The language of impedance is convenient because we can have the picture of the particle beam current circulating seeing lumped impedances at the wall of the vacuum chamber. The term $\langle F_{0s}^{\parallel} \rangle$ is the wake force on the synchronous particle. It is a constant energy loss, which is compensated by suitably choosing the synchronous phase ϕ_s .

Because of the random quantum excitation in the electron bunch, there is a finite probability of having electrons jumping outside the bucket and getting lost. To increase the *quantum lifetime* of an electron bunch, the rf bucket has to be large. Also Touschek scattering will convert transverse momentum spread of electrons into longitudinal. In order that those electrons will not be lost, the rf bucket has to be large. For this reason, the bucket in an electron machine is in general very much larger than the size of the electron

bunch, usually the height of the bucket is more than 10 times the rms energy spread of the bunch. To achieve this, the rf voltage V_{rf} for an electron ring will be relatively much larger than that in a proton ring of the same energy. Another reason of a high V_{rf} in an electron machine is to compensate for the energy loss due to synchrotron radiation. For example, in the high-energy ring of PEP II storing 9 GeV electrons, $V_{\text{rf}} = 18.5$ MV is required. On the other hand, V_{rf} for the Fermilab Tevatron storing 1 TeV protons is only 2.16 MV. As a result, the synchrotron tunes for electron rings, $\nu_s \sim 0.01$, are usually an order of magnitude larger than those for proton rings, $\nu_s \sim 0.001$. For this reason, in the consideration of collective instabilities, the synchrotron period of the protons are sometimes much longer than the instability growth times, and the proton bunches can therefore be viewed locally as coasting beams. Thus, the theory of longitudinally microwave instability, which is based on coasting beam, can be used when the average bunch current I_b is replaced by the local peak current I_{pk} . The instability can therefore be studied for each individual revolution harmonic. The stability limit is given by the Keil-Schnell criterion [2], which for a bi-Gaussian distributed bunch reads [3]

$$\left| \frac{Z_0^{\parallel}}{n} \right| < \frac{2\pi\eta E_0 \sigma_\delta^2}{e I_{\text{pk}}}, \quad (2.5)$$

where σ_δ is the rms fractional momentum or energy spread of the bunch.

2.1 MODE-MIXING INSTABILITY

For electron bunches, the synchrotron period is usually much shorter than the collective instability growth times. Thus, synchrotron oscillation cannot be neglected in the study of longitudinal instability and the coasting-beam based theory of microwave instability cannot be applied. Here, we must study the different modes of oscillation inside a bunch.

Because the beam particles execute synchrotron oscillations, it is more convenient to use circular coordinates r, ϕ in the longitudinal phase space instead. We define

$$\begin{cases} \tau = r \cos \phi, \\ p_\tau = r \sin \phi = \frac{\eta \delta}{\omega_s}, \end{cases} \quad (2.1)$$

A few azimuthal modes are shown in Fig. 2. One type of oscillation is azimuthal in ϕ , such as $\cos m\phi$. For example, $m = 1$ corresponds to a rigid dipole oscillation which we usually observe when the bunch is injected with a phase error. $m = 2$ corresponds to a quadrupole oscillation when there is a mismatch between the bunch and the rf bucket. It is clear that to drive the higher azimuthal modes, *longitudinal impedance* of higher frequencies will be required. Of course, there will also be radial modes, where the bunch oscillates with nodes at certain radii r . Let us concentrate on only one radial mode per azimuthal, the one that is most easily excited. At zero beam intensity, these modes are separated by the synchrotron frequency $\omega_s/(2\pi)$; for example, the m th mode exhibits as a sideband $m\omega_s/(2\pi)$ away from a revolution harmonic line. If the intensity of the bunch is increased, the spacings of the sidebands will change.

Here, we wish to study the collective motion of the bunch, implying that it will oscillate with a coherent

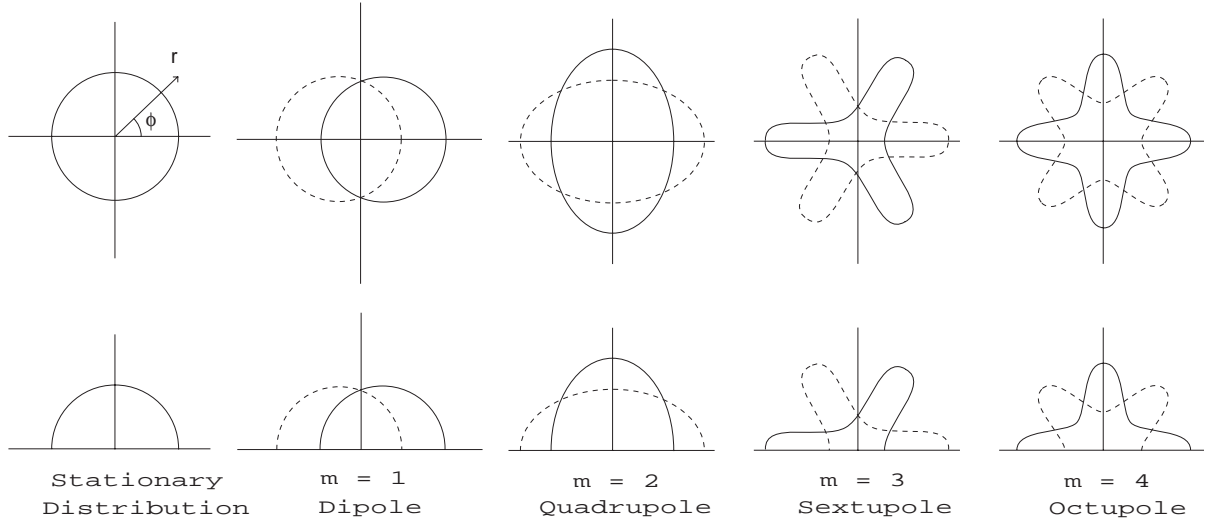


Figure 2: Azimuthal synchrotron modes of a bunch in the longitudinal phase space (top) and as linear density (bottom).

frequency $\Omega/(2\pi)$. The time dependent part is written as

$$\sum_{q=-\infty}^{\infty} F_q e^{-i(q\omega+\Omega)t}, \quad (2.2)$$

where F_q is some factor depending on q . Suppose that the synchrotron dipole mode is excited, we will have $\Omega \approx +\omega_s$, provided that the intensity of the bunch is not too large. Therefore, the spectrum of the bunch will consist of only *upper* synchrotron sidebands at a distance ω_s above the harmonic line, as shown in the top plot of Fig. 3. Of course, not all the sidebands will be excited equally. The excitation will depend on the driving impedance and also the bunch shape. However, in an oscilloscope or network analyzer, we can see only *positive* frequencies. This is equivalent to folding the spectrum about the zero frequency point, the upper synchrotron sidebands corresponding to the negative harmonics will appear as lower synchrotron sidebands for the positive frequencies, or the lower plot of Fig. 3. When the driving impedance is a narrow resonance, we may have $\Omega \approx -\omega_s$ instead. However, notice that $\text{Re} Z_0^{\parallel}$ is even in frequency, or $\text{Re} Z_0^{\parallel}(\omega) = \text{Re} Z_0^{\parallel}(-\omega)$. There for $\omega_r = q\omega_0 - \omega_s$, where $\omega_r/(2\pi)$ is resonant frequency of the impedance and $q > 0$, we can always write $-\omega_r = q'\omega_0 + \omega_s$ with $q' = -q$. The conclusion is that for longitudinal collective motion, it is suffice to study only the situation of having the coherent frequency $\Omega \approx +\omega_s$. In other words, we can assume all the synchrotron sidebands to be only upper sidebands in the language of having both positive and negative frequencies. This analysis, however, is not correct for transverse collective motion.

Assume a broad-band impedance resonating at ω_r . The impedance will be inductive when $\omega < \omega_r$ and capacitive when $\omega > \omega_r$. If the rms length of the bunch $\sigma_{\tau} > \omega_r^{-1}$, the bunch particles are seeing mostly the inductive part of the impedance. Because the beam particles are traveling at the velocity of light in a

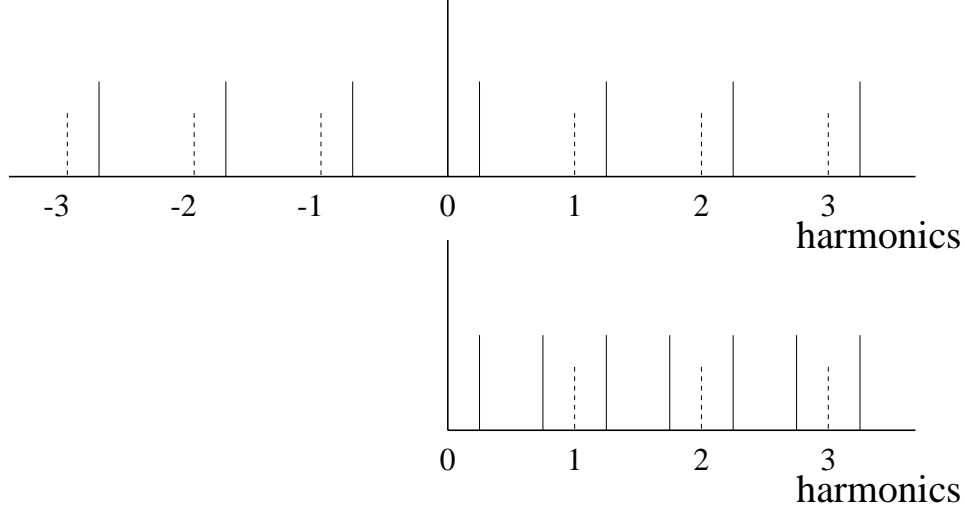


Figure 3: Top plot shows the synchrotron lines for both positive and negative revolution harmonics. The revolution harmonics are shown in dashes and the synchrotron *upper* sidebands in solid. Lower plot shows the negative-harmonic side folded onto the positive-harmonic side. We see upper and lower sideband for each harmonic line.

ring with positive momentum compaction, this inductive force is repulsive opposing the focusing force of the rf voltage, thus lengthening the bunch and lowering the synchrotron frequency. Therefore, all azimuthal modes will be shifted downward, except for the dipole mode $m = 1$. This is because the centroid of the bunch does not see any reactive impedance. When the bunch intensity is large enough, the $m = 2$ mode will collide with the $m = 1$ mode, and an instability will occur if the frequencies corresponding to these two modes fall inside the resonant peak of $\text{Re } Z_0^{\parallel}$. Mathematically, the frequency shifts become complex. This is called longitudinal mode-mixing instability. An illustration is shown in Fig. 4 for a parabolic bunch of full length τ_L interacting with a broad band impedance resonating with impedance R at frequency $\omega_r/(2\pi)$. A rough threshold can be derived by, for example, equating the shift to ω_s . It happens to be roughly the same as the Keil-Schnell criterion in Eq. (2.5), except that the left side is replaced by

$$\left| \frac{Z_0^{\parallel}}{n} \right| \longrightarrow \left. \frac{Z_0^{\parallel}}{n} \right|_{\text{eff}} = \frac{\int d\omega \frac{Z_0^{\parallel}(\omega)}{\omega} \omega_0 h_m(\omega)}{\int d\omega h_m(\omega)}, \quad (2.3)$$

where $h_m(\omega)$ is the power spectrum of the m th azimuthal mode depicted in the bottom plots of Fig. 2. For this reason, this instability is also called microwave instability. The signal measured should correspond roughly to the rms frequency of the bunch spectrum, which is also in the microwave region because an electron bunch is often shorter than the transverse size of the vacuum chamber. For Sacherer's approximate sinusoidal modes, the power spectra of some lower azimuthal modes are shown in Fig. 5.

2.2 BUNCH LENGTHENING AND SCALING LAW

If the bunch length $\sigma_{\tau} < \omega_r^{-1}$, the bunch particles will sample mostly the capacitive part of the broad-

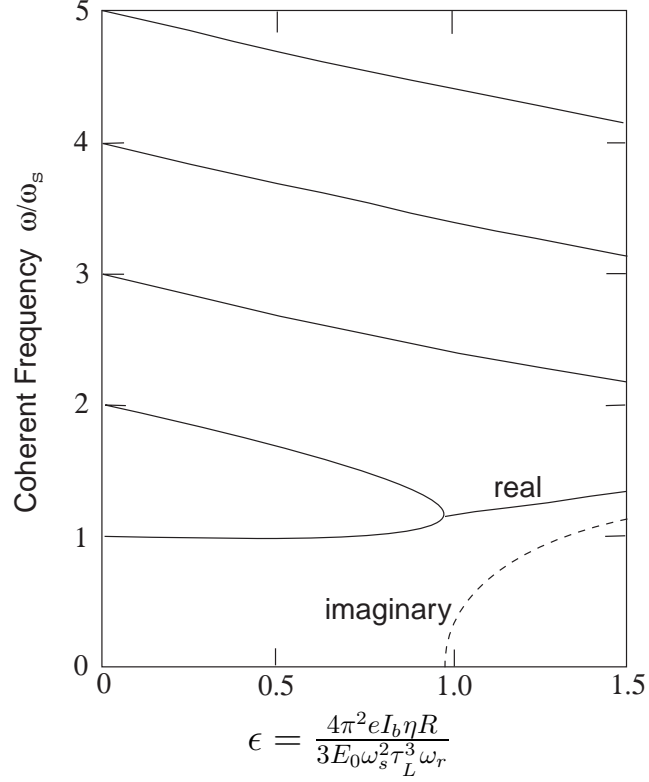


Figure 4: Plot showing longitudinal mode-mixing instability of a parabolic bunch of full length τ_L interacting with a broad band impedance resonating with impedance R at frequency $\omega_r/(2\pi)$. The bunch length τ_L is much longer than ω_r^{-1} so that the bunch particles are seeing the inductive part of the impedance. Thus, all modes, except for $m = 1$, shift downward.

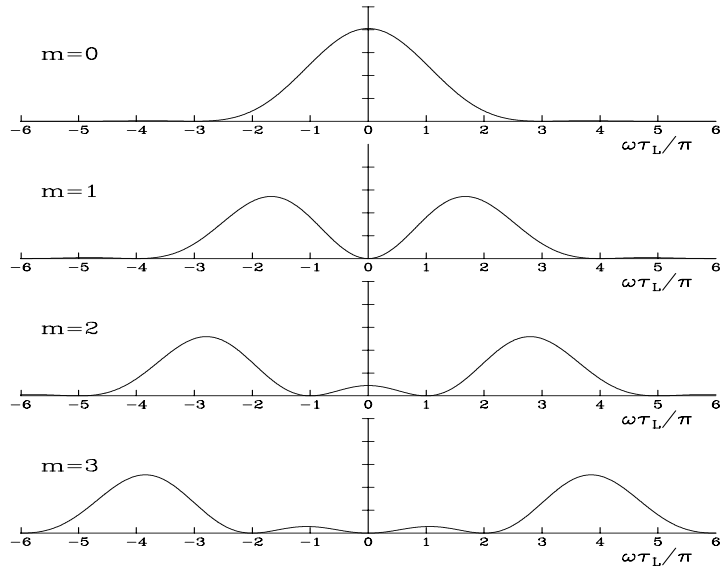


Figure 5: Power spectra $h_m(\omega)$ for modes $m = 0$ to 3 with zero chromaticity.

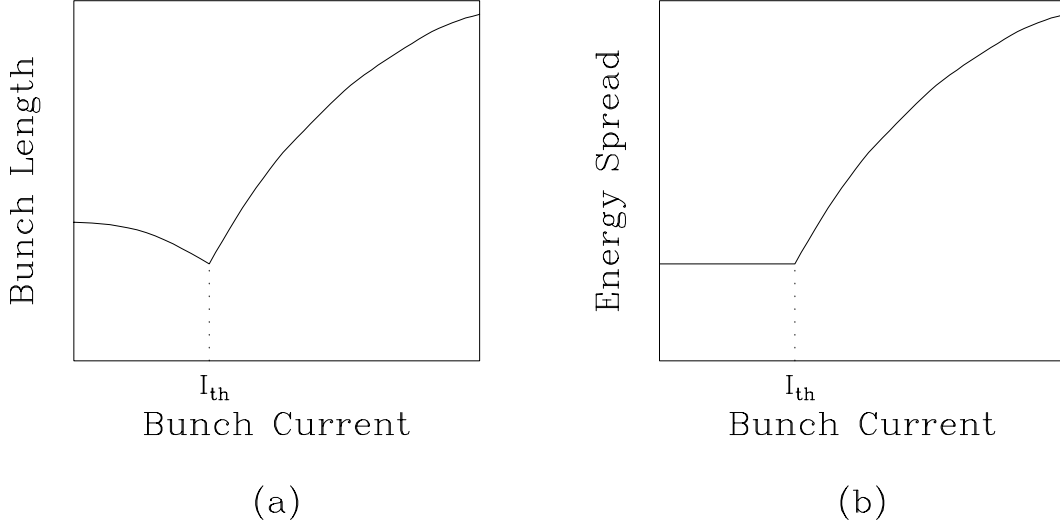


Figure 6: Both the bunch length and energy spread begin to grow after the bunch current exceeds its microwave instability threshold I_{th} . (a) The bunch length starts with its natural value at zero current and becomes shortened due to the capacitive potential-well distortion. (b) Below the instability threshold, the energy spread is always at its natural value unaffected by the effect of potential-well distortion.

band impedance. The frequencies of the azimuthal modes will shift upward instead. It will therefore be harder for the $m = 2$ and $m = 1$ modes to collide, the threshold will be relatively higher. Typical plots of the bunch length and energy spread are shown in Fig. 6. Note that because of the balancing of synchrotron radiation and random quantum excitation, there is a *natural* momentum spread σ_{δ_0} and the corresponding natural bunch length σ_{τ_0} is determined by the rf voltage. This is what we see below the threshold. As the bunch intensity increases, the bunch length decreases because of the *attractive* capacitive impedance. This is called *potential-well distortion*. However, the momentum spread is still determined by its natural value and is not changed. Unlike a proton bunch which can be lost after the microwave instability threshold, the electron bunch can stabilize itself by self-increasing its length and energy spread, as illustrated in Fig. 6. One way to observe this instability is to measure the increase in bunch length. We can also monitor the synchrotron sidebands and see the $m = 2$ sideband approach the $m = 1$ sideband. This frequency shift, which is a coherent shift, as a function of beam intensity is a measure of the reactive impedance of the ring. An accurate measurement of the frequency shift of the $m = 2$ mode may sometimes be difficult. An alternate and more accurate determination of the frequency shift can be made by monitoring the phase shift in the beam transfer function.

There is a scaling law relating the bunch lengthening and the frequency dependency of the impedance sampled by the bunch. It says that the rms bunch length σ_τ above threshold depends on only one parameter

$$\xi = \frac{\eta I_b}{\nu_s^2 E_0}, \quad (2.1)$$

as

$$\sigma_\tau \propto \xi^{1/(2+a)} \quad (2.2)$$

when the part of the impedance sampled by the bunch behaves like

$$Z_0^{\parallel} \propto \omega^a . \quad (2.3)$$

Here, I_b is the average beam current of the bunch. This scaling law was first derived by Chao and Gareyte [4] and has been verified experimentally. Note that if the Keil-Schnell criterion is applied, we always have $\sigma_{\tau} \propto \xi^{1/3}$ or $a = 1$, implying a long bunch seeing the inductive part of the impedance. However, for SPEAR, measurement pointed to $\sigma_{\tau} \propto \xi^{0.76}$ or $a = -0.68$. This clearly demonstrates that the Keil-Schnell criterion cannot be used in an electron machine where the synchrotron period is short. There is another big difference between the microwave instability for coasting beam and the mode-mixing instability discussed here. Above transition, which is true for nearly all electron rings, the tear-drop stability curve of the coasting-beam based theory states that the beam will be unstable if it is driven by a capacitive impedance which is large enough. However, it can be shown that pure reactive impedance cannot lead to mode-mixing instability. The modes may cross each other due to frequency shifts but no instability will materialize.

This instability is not a devastating instability, because it results only in the blowup of the bunch area. In fact, many storage rings, especially collider rings, operate above this threshold, because a much higher beam intensity and therefore luminosity can be attained. However, this may not be the situation for a light source, where we always want to shorter bunches so as to have smaller spot sizes for the synchrotron light. In order to accomplish this the electron ring must be carefully designed so that the impedance is as small as possible. On the other hand, it is very difficult to reduce the impedance in a ring already built. For example, some capacitive structures had been placed in the SLAC damping ring, so as to reduce the inductive impedance of the ring. The threshold of the mixing of the $m = 2$ and $m = 1$ mode has been actually pushed higher. However, the beam particles are now seeing mostly the real part of the impedance, which distorts the bunch asymmetrically bringing out the importance of other radial excitation modes. These radial modes actually collide at a threshold much lower than the previously threshold before the modification. However, this instability due to the mixing of radial modes are much weaker than the instability due to the mixing of azimuthal modes.

2.3 SAWTOOTH INSTABILITY

Before the modification of the vacuum chamber SLAC damping ring, a new form of longitudinal instability coupling with synchrotron radiation damping was observed. Upon the injection of a bunch, the bunch length decreased rapidly with a longitudinal damping time of the order of 2 ms. When the bunch length passed below a threshold, a sudden blowup in bunch length occurred in a time span comparable to or shorter than the 10 μ s synchrotron period, as illustrated in Fig. 7. This process was self limiting because of the nonlinear nature of the short range wake fields responsible for blowing up the bunch. Since the blowup is faster than a synchrotron period, this might have been the type of coasting-beam based microwave instability governed by the Boussard-modified Keil-Schnell criterion. Once the blowup ceased, the bunch damped down until the threshold was reached again in about a synchrotron damping time of ~ 1.3 ms. Thus, a cyclical repetition of the instability was observed and termed according to its shape *saw-tooth instability* [5].

The time dependent nature was seen in the bunch-length signal from the Beam Position Monitor (BPM) electrodes and the bunch-phase signal from the synchronous phase monitor. The bunch phase can

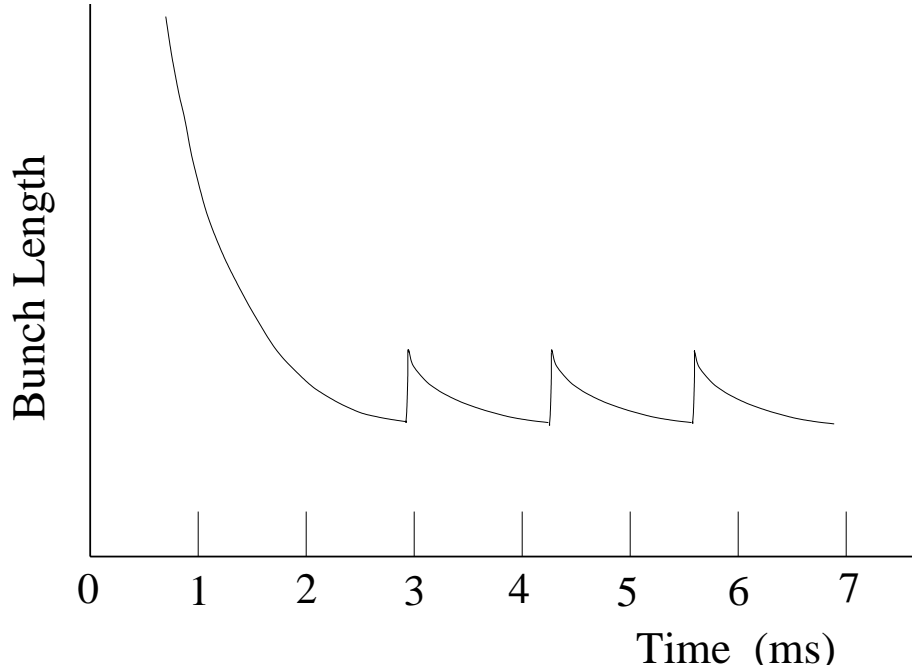


Figure 7: Plot of bunch length versus time at the injection of the SLAC Damping ring with an intensity of 3×10^{10} particles per bunch. The bunchlength was damped rapidly in the first 2 ms after injection to a point where it was unstable against microwave instability. Rapid growth took place until the bunch was self-stabilized. After that it was damped by synchrotron radiation to below the instability threshold. This repetition has the shape of sawteeth.

be referenced to either the 714 MHz rf of the damping ring or to the 2856 MHz S-band rf of the linac. The synchronous beam phase angle is given by $\phi_s = \sin^{-1}(U_0/V_{\text{rf}})$, where U_0 is the energy loss per turn as a result of synchrotron radiation. The higher-order mode losses of a bunch is a function of the line charge density and so are inversely proportional to the bunch length. As the bunch blew up, the higher-order losses decreased and the beam phase shifted by about 0.5° at 714 MHz during a saw-tooth. This translated into a 2° jump at the S-band in the linac. This magnitude of phase error caused a problem with the rf bunch length compressor in the ring-to-linac beam line. When this instability took place, the bunch would be incorrectly launched into the linac and might eventually be lost on the downstream collimators, causing the linac to trip the machine protection circuits.

This instability can also be observed in the frequency domain. As the beam was damped down to the instability threshold, strong signal appeared at the $3\nu_s$ sideband, corresponding to a sextupole mode of oscillation in the bunch length. Although this sideband was referred to as $3\nu_s$, its frequency was depressed from 3 times to ~ 2.6 times.

There is a threshold for this instability, which occurred at around 3×10^{10} particles per bunch for a nominal rf voltage of 1 MV. At higher intensity, the sawteeth appeared closer together in time. The process could be viewed as a relaxation oscillator where the period is a function of the bunch length damping time

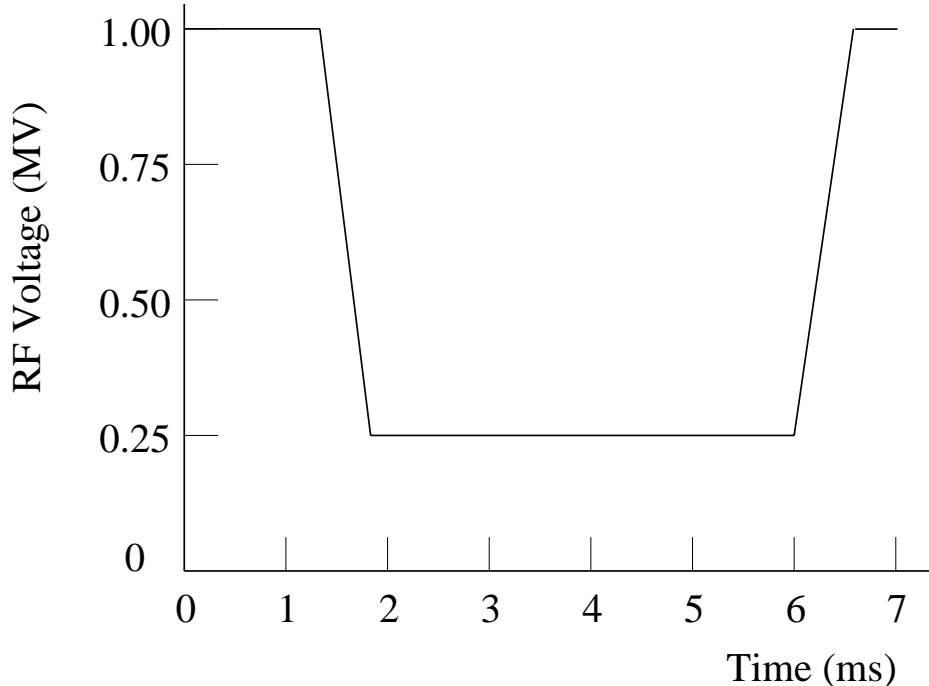


Figure 8: The rf voltage was lowered in the SLAC damping ring after injection and before extraction, thus lengthening the bunch and reducing the local charge density. This raised the microwave instability threshold and prevented the sawtooth instability.

and the trigger threshold. The damping time is constant but the bunch length at which the bunch went unstable increased at higher intensities. When the bunch intensity was increased to 4×10^{10} particles, a transition occurred to a second regime with “continuous sawteeth”.

Lowering the rf voltage is a means of increasing the equilibrium bunch length and extending the intensity threshold. This is because the Landau damping from the energy spread, which is determined by synchrotron radiation, is unchanged, but lengthening the bunch reduces the local peak current and brings the bunch below the Keil-Schnell threshold according to Eq. (2.5). A low rf voltage, however, is not suitable for efficient injection and extraction for the damping ring. Therefore, the rf voltage was ramped down from 1 MV to 0.25 MV approximately 1 ms after injection, as illustrated in Fig. 8. It was ramped up back to 1 MV 0.5 ms before extraction. In this way the onset of saw-tooth instability had been suppressed up to an intensity of 3.5×10^{10} per bunch.

3 ROBINSON INSTABILITY

When an off-momentum particle executes synchrotron oscillation in the longitudinal τ - ΔE plane, its energy oscillates. In the upper half plane, its instantaneous revolution frequency is $\omega_0(1-\eta\delta)$ which is smaller than ω_0 , whereas in the lower half plane, its revolution frequency is larger than ω_0 . Consider the $\text{Re } Z_0^{\parallel}$ near a revolution harmonic $q\omega_0$. If $\text{Re } Z_0^{\parallel}$ is smaller at $q\omega_0 + \omega_s$ than at $q\omega_0 - \omega_s$, the particle will be losing

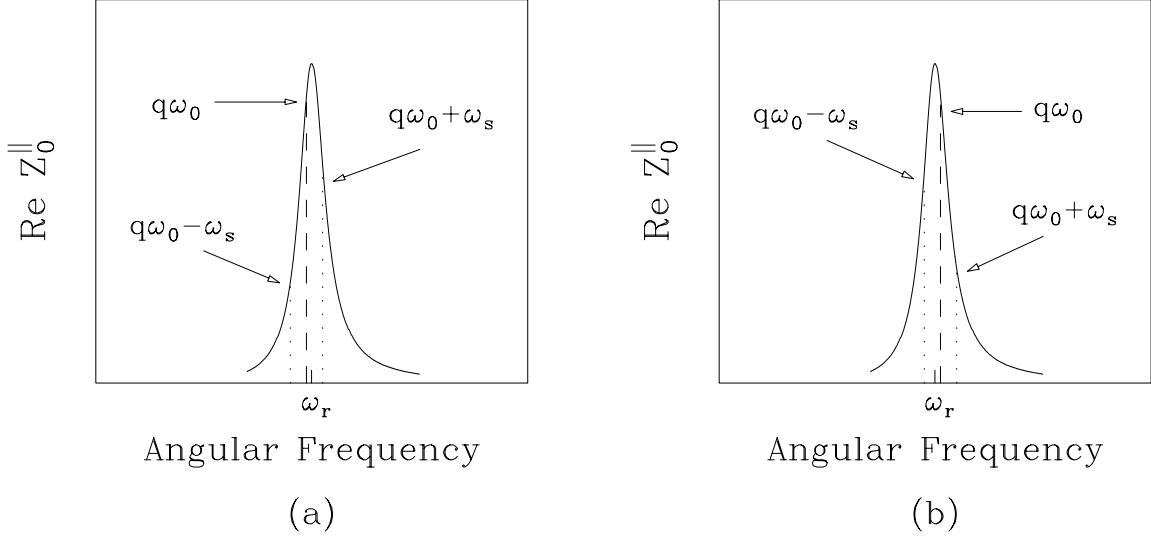


Figure 9: (a) If the resonant frequency ω_r is slightly above a revolution harmonic $q\omega_0$, $\text{Re } Z_0^{\parallel}$ at the upper synchrotron sideband is larger than at the lower synchrotron sideband. The system is unstable. (b) If ω_r is slightly below a harmonic line, $\text{Re } Z_0^{\parallel}$ at the upper sideband is smaller than at the lower sideband, and the system is stable. It is the other way around if the operation is below transition.

energy in the upper half plane when $\delta > 0$ and gaining energy in the lower half plane when $\delta < 0$. Thus, the synchrotron oscillation amplitude will be reduced, and the oscillation will be damped. This is illustrated in Fig. 9(b). On the other hand, if $\text{Re } Z_0^{\parallel}$ is larger at $q\omega_0 + \omega_s$ than at $q\omega_0 - \omega_s$, as indicated in Fig. 9(a), the oscillation will be unstable because the amplitude will become larger and larger. This instability criterion was first analyzed by Robinson [6].

Since we require a rapid change of $\text{Re } Z_0^{\parallel}$ as a function of frequency in order to exhibit Robinson damping or Robinson anti-damping, this $\text{Re } Z_0^{\parallel}$ is usually a sharp resonance, for example the fundamental rf resonance. Thus, in order that synchrotron oscillation is stable, the resonant rf frequency ω_r must be tuned so that it is slightly below a revolution harmonic. For proton machines below transition where the slip factor $\eta < 0$, the opposite is necessary to ensure stability or ω_r must be slightly above a revolution harmonic.

Narrow resonant impedance peak implies long wake function, so long that the particle will see its own wake left in previous turns. Including the contribution of the wake due to previous turns in the energy-change equation of motion [Eq. (1.4)], one can derive the growth rate as the imaginary part of the synchrotron tune shift:

$$\frac{1}{\tau_m} = \text{Im } \Delta\omega_s = \frac{\eta e I_b}{2E_0 T_0 \omega_s} \sum_{q=-\infty}^{+\infty} (q\omega_0 + m\omega_s) \text{Re } Z_0^{\parallel}(q\omega_0 + m\omega_s) F_m(q\omega_0 + m\omega_s), \quad (3.1)$$

where I_b is the average bunch current, $m = 1$ is the dipole mode, $m = 2$ is the quadrupole mode, etc. In above, F_m is a form factor depending on the linear distribution of the bunch. Take the simple case of a

single bunch of length $2\hat{\tau}$ and uniform distribution in the longitudinal phase space, or

$$g_0(r) = \frac{1}{\pi\hat{\tau}^2} \theta(\hat{\tau} - r) , \quad (3.2)$$

where $\theta(x) = 1$ when $x > 0$ and zero otherwise. The form factor becomes

$$F_m(\omega) = \frac{1}{\pi\hat{\tau}^2} J_m^2(\omega\hat{\tau}) \approx \frac{\omega^2}{4\pi} \frac{1}{(m!)^2} \left(\frac{\omega\hat{\tau}}{2}\right)^{2m-2} , \quad (3.3)$$

where the assumption of a short bunch has been made in the last step. Therefore for the dipole mode ($m = 1$), $F \approx 1$ and is independent of the bunch length if the bunch is short. In other words, the dipole mode of a short bunch is essentially a point-bunch theory. It is worthwhile to point out that the form factor F_m is in fact another way to express the power spectrum h_m of the m th azimuthal excitation illustrated in Fig. 5.

When the driving impedance is a resonance centered at frequency $\omega_r/(2\pi)$ and is so narrow that there is only one $q > 0$ that satisfies

$$\omega_r \approx q\omega_0 \pm \omega_s , \quad (3.4)$$

only two terms of the above summation survive. The growth rate becomes, for the dipole mode,

$$\frac{1}{\tau_1} = \frac{\eta e I_b \omega_r}{2 E_0 T_0 \omega_s} [\text{Re } Z_0^{\parallel}(q\omega_0 + \omega_s) - \text{Re } Z_0^{\parallel}(q\omega_0 - \omega_s)] . \quad (3.5)$$

The result agrees with the illustration in Fig. 9. From Fig. 3 where we have upper and lower synchrotron sidebands in the language of positive frequencies, it is now easy to explain the different contributions of the upper and lower synchrotron sidebands to collective stability of the beam particles. In the situation of electron rings where the slip factor $\eta > 0$, we can therefore identify, according to Eq. (3.5), the upper sidebands as the growing sidebands and the lower sidebands the damping sidebands.

Experimental observation of Robinson instability is easy, because one can identify a growing amplitude of the synchrotron oscillation amplitude in the time domain. In the frequency domain, one can observe the upper synchrotron sideband of the rf harmonic growing in strength. As was discussed above, detuning the rf frequency to slightly below a revolution harmonic will achieve Robinson damping. In addition, there is also Landau damping coming from the spread of the synchrotron frequency inside the bunch resulting from, for example, the nonlinearity of the rf wave. As a rule of thumb, the stability criterion reads

$$\frac{1}{\tau_1} < \frac{1}{\sqrt{3}} \Delta\omega_{1/2} . \quad (3.6)$$

where $\Delta\omega_{1/2}$ is the half spread of the synchrotron frequency at half maximum.

4 LONGITUDINAL COUPLED-BUNCH INSTABILITY

4.1 COUPLED MODES AND GROWTH RATES

When the wake does not decay within the bunch spacing, bunches talk to each other. Assuming M bunches of equal intensity equally spaced in the ring, there are $\mu = 0, 1, \dots, M-1$ modes of oscillations in

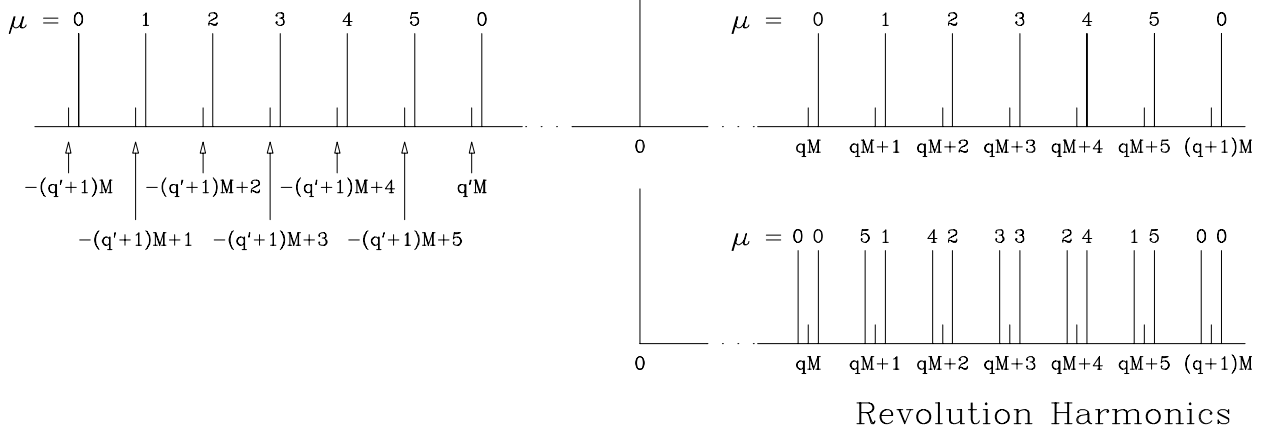


Figure 10: Top plot shows the synchrotron lines for both positive and negative revolution harmonics for the situation of $M = 6$ identical equally-spaced bunches. The coupled-bunch modes $\mu = 0, 1, 2, 3, 4, 5$ are listed at the top of the synchrotron lines. Lower plot shows the negative-harmonic side folded onto the positive-harmonic side. We see upper and lower sideband for each harmonic line.

which the center-of-mass of a bunch *leads*[†] its predecessor by the phase $2\pi\mu/M$. In addition, an individual bunch in the μ -th coupled-bunch mode can oscillate in the synchrotron phase space about its center-of-mass in such a way that there are $m = 1, 2, \dots$ azimuthal nodes in the perturbed longitudinal phase-space distribution. Of course, there will be in addition radial modes of oscillation in the perturbed distribution. The long-range wake can drive the coupled bunches to instability.

For M equal bunches, Eq. (3.5) becomes, for coupled-bunch mode μ ,

$$\frac{1}{\tau_{1\mu}} = \frac{\eta e I_b M \omega_r}{2\beta^2 E_0 T_0 \omega_s} [\text{Re } Z_0^{\parallel}(qM\omega_0 + \mu\omega_0 + \omega_s) - \text{Re } Z_0^{\parallel}(q'M\omega_0 - \mu\omega_0 - \omega_s)] , \quad (4.1)$$

where I_b is the average current for *one* bunch. When $\mu = 0$, both terms will contribute with $q' = q$ and we have exactly the same Robinson's stability or instability as for the single bunch situation. This is illustrated in Fig. 10. When $\mu = M/2$ if M is even, both terms will contribute with $q' = q$, and the same Robinson's stability or instability will apply. For the other $M-2$ modes, only one term will be at or close to the resonant frequency and only one term will contribute. If the positive-frequency term contributes, we have instability. If the negative-frequency term contributes, we have damping instead. If one choose to speak in the language of only positive frequencies, there will be an upper and lower synchrotron sideband surrounding each revolution harmonic. Above transition, the coupled-bunch system will be unstable if the driving resonance leans towards the upper sideband and stable if it leans towards the lower sideband.

For the higher azimuthal modes ($m > 1$) driven by a narrow resonance, we have the same Robinson instability. The growth rates are

$$\frac{1}{\tau_{m\mu}} = \frac{\eta e^2 N M \omega_r}{2\beta^2 E_0 T_0^2 \omega_s} \frac{m}{(m!)^2} \left(\frac{\omega_r \hat{\tau}}{2}\right)^{2m-2} [\text{Re } Z_0^{\parallel}(qM\omega_0 + \mu\omega_0 + \omega_s) - \text{Re } Z_0^{\parallel}(q'M\omega_0 - \mu\omega_0 - \omega_s)] , \quad (4.2)$$

[†]We can also formulate the problem by having the bunch *lags* its predecessor by the phase $2\pi\mu'/M$ in the μ' -th coupling mode. Then mode μ' will be exactly the same as mode $M-\mu$ discussed in the text.

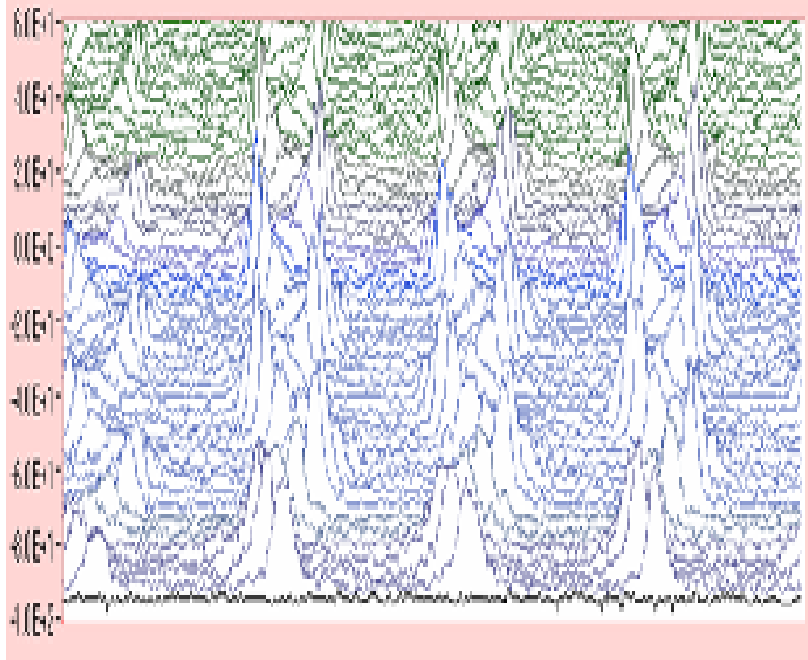


Figure 11: (color) Mountain-range plot showing coupled-bunch instability in the Fermilab Main Injector just after injection at 8 GeV.

which depend on the bunch length as $\hat{\tau}^{2m-2}$, where the form factor F in Eq. (3.3) for a short but uniform distributed bunch has been used. As a result, higher azimuthal instabilities for short bunches will be much more difficult to excite.

The easiest way to observe longitudinal coupled-bunch instability is in mountain-range plot, where bunches oscillate in a particular pattern as time advances. Examples are shown in Figs. 11 and 12. Streak camera can also be used to capture the phases of adjacent bunches as a function of time. From the pattern of coupling, the coupled-mode μ can be determined. From the frequency of oscillation, the azimuthal mode m can also be determined. Then we can pin down the frequency $\omega_r/(2\pi)$ of the offending resonance driving the instability.

Observation can also be made in the frequency domain by zooming in the region between two rf harmonics in the way illustrated in Fig. 10. The coupled-bunch mode excited will be shown as a strong spectral line in between.

Longitudinal coupled-bunch instability will lead to an increase in bunch length and an increase in energy spread. For a light source, this translates into an increase in the spot size of the synchrotron light.

There are many way to cure longitudinal coupled bunch instability. The driving resonances are often the higher order modes inside the rf cavities. When the particular resonance is identified and if it is much narrower than the revolution frequency of the ring, we can try to shift its frequency so that it resides in between two revolution harmonics and becomes invisible to the beam particles. We can also study the

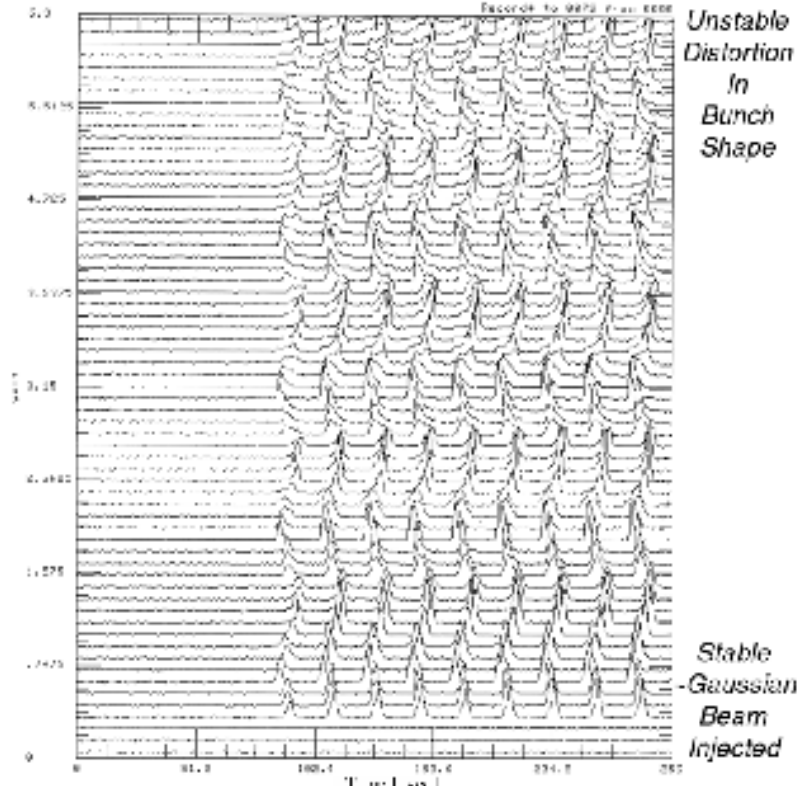


Figure 12: (color) Mountain range plot showing bunches in a batch executing coupled-bunch instability in the Fermilab Main Injector just after injection at 8 GeV

electromagnetic field pattern of this resonance mode inside the cavity and install passive resistors and antenna to damp this particular mode. This method has been used widely in the Fermilab Booster, where longitudinal coupled-bunch instability had been very severe after the beam passed the transition energy. At that time, the bunch area increased almost linearly with bunch intensity. Passive damping of several offending modes cured this instability to such a point that the bunch area does not increase with bunch intensity anymore.

Longitudinal coupled-bunch instability had also been observed in the former Fermilab Main Ring. Besides passive damping of the cavity resonant modes, the instability was also reduced by lowering the rf voltage. Lowering the rf voltage will lengthen the bunch and reduce the form factor F . This is only possible for a proton machine where the bunches are long. It will not work for the short electron bunches for the $m = 1$ dipole mode. This is because, as mentioned before, the form factor for the dipole mode is not sensitive to the bunch length for short bunches. Even for a proton machine, the rf voltage cannot be reduced by a large amount because, proton bunches are usually rather tight inside the rf bucket, especially during ramping.

If the growth turns out to be harmful, a fast bunch-by-bunch damper may be necessary to damp the dipole mode ($m = 1$). A damper for the quadrupole mode ($m = 2$) may also be necessary. This consists essentially of a wall-gap pickup monitoring the changes in bunch length and the corresponding excitation of a modulation of the rf waveform with roughly twice the synchrotron frequency. A feed-back correction is then made to the rf voltage. Another way to damp the longitudinal coupled-bunch instability is to break

the symmetry between the M bunches. For example, a 5% to 10% variation in the intensity of the bunches will help. Also the bunches are usually not placed symmetrically in the ring. Some analysis shows that the stability will be improved if some bunches in the symmetric configuration are missing.

There can also be Landau damping, which comes from the spread of the synchrotron frequency. The spread due to the nonlinear sinusoidal rf wave form can be written as

$$\frac{\Delta\omega_s}{\omega_s} = \frac{2}{3} \left(\frac{1 + \sin^2 \phi_s}{1 - \sin^2 \phi_s} \right) \left(\frac{h\tau_L \omega_0}{4\pi} \right)^2, \quad (4.3)$$

where τ_L is the total length of the bunch and ϕ_s is the synchronous angle. The mode will be stable if

$$\frac{1}{\tau} \lesssim \frac{\sqrt{m}}{4} \Delta\omega_s. \quad (4.4)$$

Electron bunches are usually much smaller in size than the rf bucket. As a result the spread in synchrotron frequency will be very minimal, and does not help much in Landau damping.

4.2 HIGHER-HARMONIC CAVITIES

In order to Landau damp longitudinal coupled-bunch instability, a large spread in synchrotron frequency inside the bunch must be required. One way to do this is to install a higher-harmonic cavity, sometime known as *Landau cavity* [7]. For example, the higher-harmonic cavity has resonant frequency $m\omega_{\text{rf}}$, where ω_{rf} is the resonant frequency of the fundamental rf cavity. The total rf voltage seen by the beam particles becomes

$$V(\tau) = V_{\text{rf}}[\sin(\phi_s - \omega_{\text{rf}}\tau) + k \sin(\phi_m - m\omega_{\text{rf}}\tau)] \quad (4.1)$$

We would like the bottom of the potential well, which is the integral of $V(\tau)$, to be as flat as possible. The rf voltage seen by the synchronous particle is compensated to zero by the energy lost to synchrotron radiation. Therefore, if we further require

$$\left. \frac{\partial V}{\partial \tau} \right|_{\tau=0} = 0, \quad \text{and} \quad \left. \frac{\partial^2 V}{\partial \tau^2} \right|_{\tau=0} = 0. \quad (4.2)$$

so that the potential will become quartic instead. The above translates into

$$\cos \phi_s = -km \cos \phi_m \quad \text{and} \quad \sin \phi_s = -km^2 \sin \phi_m, \quad (4.3)$$

from which ϕ_m and k can be solved easily. For small amplitude oscillation, the potential becomes

$$-\int V(\tau) d(\omega_{\text{rf}}\tau) \longrightarrow \frac{m^2 - 1}{24} (\omega_{\text{rf}}\tau)^4 V_{\text{rf}} \cos \phi_s, \quad (4.4)$$

and the synchrotron frequency

$$\frac{\omega_s(\tau)}{\omega_{s0}} = \frac{\pi}{2} \left(\frac{m^2 - 1}{6} \right)^{1/2} \frac{\omega_{\text{rf}}\tau}{K_0}. \quad (4.5)$$

where ω_{s0} is the synchrotron frequency at zero amplitude when the higher-harmonic cavity voltage is turned off, and $K_0 = 1.854$ is the complete elliptic integral of the first kind with argument 1/2. The synchrotron frequency is zero at zero amplitude and increases linearly with amplitude. This large spread in synchrotron

frequency may be able to supply ample landau damping to the longitudinal coupled-bunch instability, A third-harmonic harmonic cavity has been used in the SOLEIL ring in France to give a relative frequency spread of about 200%. However, since the center frequency has been dramatically decreased (not exactly to zero), the net result is a poor improvement in the stabilization. The gain in the stability threshold has been only 30% [8]. [13]

4.3 RF VOLTAGE MODULATION

The modulation of the rf system will create nonlinear parametric resonances, which redistribute particles in the longitudinal phase plane. The formulation of islands within an rf bucket reduces the density in the bunch core. As a result, beam dynamics property related to the bunch density, such as beam life time, beam collective instabilities, etc, can be improved.

Here we try to modulate the rf voltage with a frequency $\nu_m\omega_0/(2\pi)$ and amplitude ϵ , so that the energy equation becomes [9]

$$\frac{d\Delta E}{dn} = eV_{\text{rf}}[1 + \epsilon \sin(2\pi\nu_m n + \xi)][\sin(\phi_s - h\omega_0\tau) - \sin\phi_s] - [U(\delta) - U_s] , \quad (4.1)$$

where ξ is a randomly chosen phase and ν_m the modulating tune. This modulation will introduce resonant island structure in the longitudinal phase plane. There are two critical tunes:

$$\begin{cases} \nu_1 = 2\nu_s + \frac{1}{2}\epsilon\nu_s , \\ \nu_2 = 2\nu_s - \frac{1}{2}\epsilon\nu_s . \end{cases} \quad (4.2)$$

If we start the modulation by gradually increasing the modulating tune ν_m towards ν_2 from below, two islands appear inside the bucket from both sides, as shown in the second plot of Fig. 13. The phase space showing the islands is depicted in Fig. 14. As ν_m is increased, these two islands come closer and closer to the center of the bucket and the particles in the bunch core gradually spill into these two islands, forming 3 beamlets. When ν_m reaches ν_2 , the central core disappears and all the particles are shared by the two beamlets in the two islands. Further increase of ν_m above ν_2 moves the two beamlets closer together. When ν_m equals ν_1 , the two beamlets merge into one. Under all these situations, the two outer islands rotate around the center of the rf bucket with frequency equal to one half the modulation frequency.

Rf voltage modulation has been introduced into the light source SRRC at Taiwan to cope with longitudinal coupled-bunch instability [10]. A modulation frequency slightly below twice the synchrotron frequency with 10% voltage modulation was applied to the rf system. The beam spectrum measured from the BPM sum from a HP4396A network analyzer before and after the modulation is shown in Fig. 15. It is evident that the intensity of the beam spectrum has been largely reduced after the application of the modulation. The sidebands around the harmonics of 587.106 Hz and 911.888 MHz are magnified in Fig. 16. We see that the synchrotron sidebands have been suppressed by very much. The multibunch beam motion under rf voltage modulation was also recorded by streak camera, which did not reveal any coupled motion of the bunches.

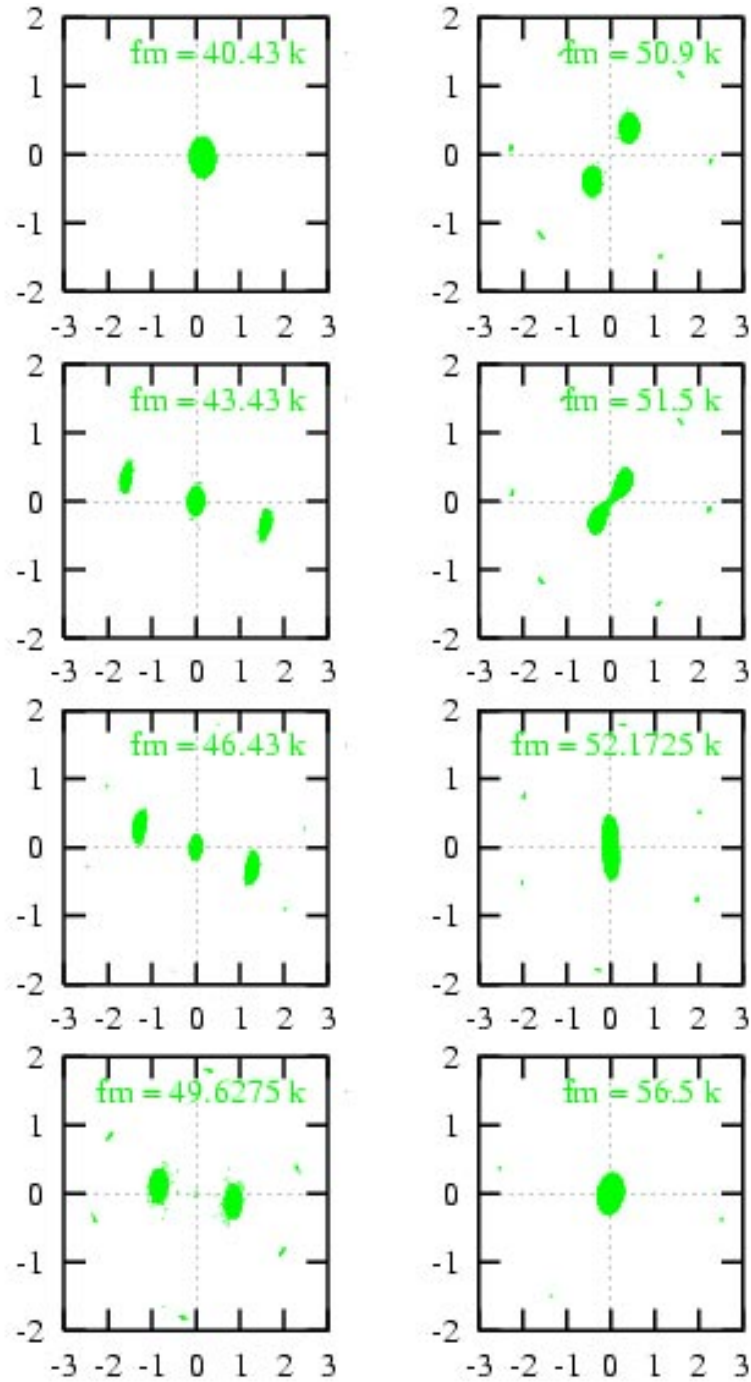


Figure 13: (color) Simulation results of rf voltage modulation. The modulation frequency is increased from top to bottom and left to right. The modulation amplitude is 10% of the cavity voltage. The 4th plot is right at critical frequency $\nu_2 f_0 = 49.6275 \text{ kHz}$ and the 7th plot right at critical frequency $\nu_1 f_0 = 52.1725 \text{ kHz}$.

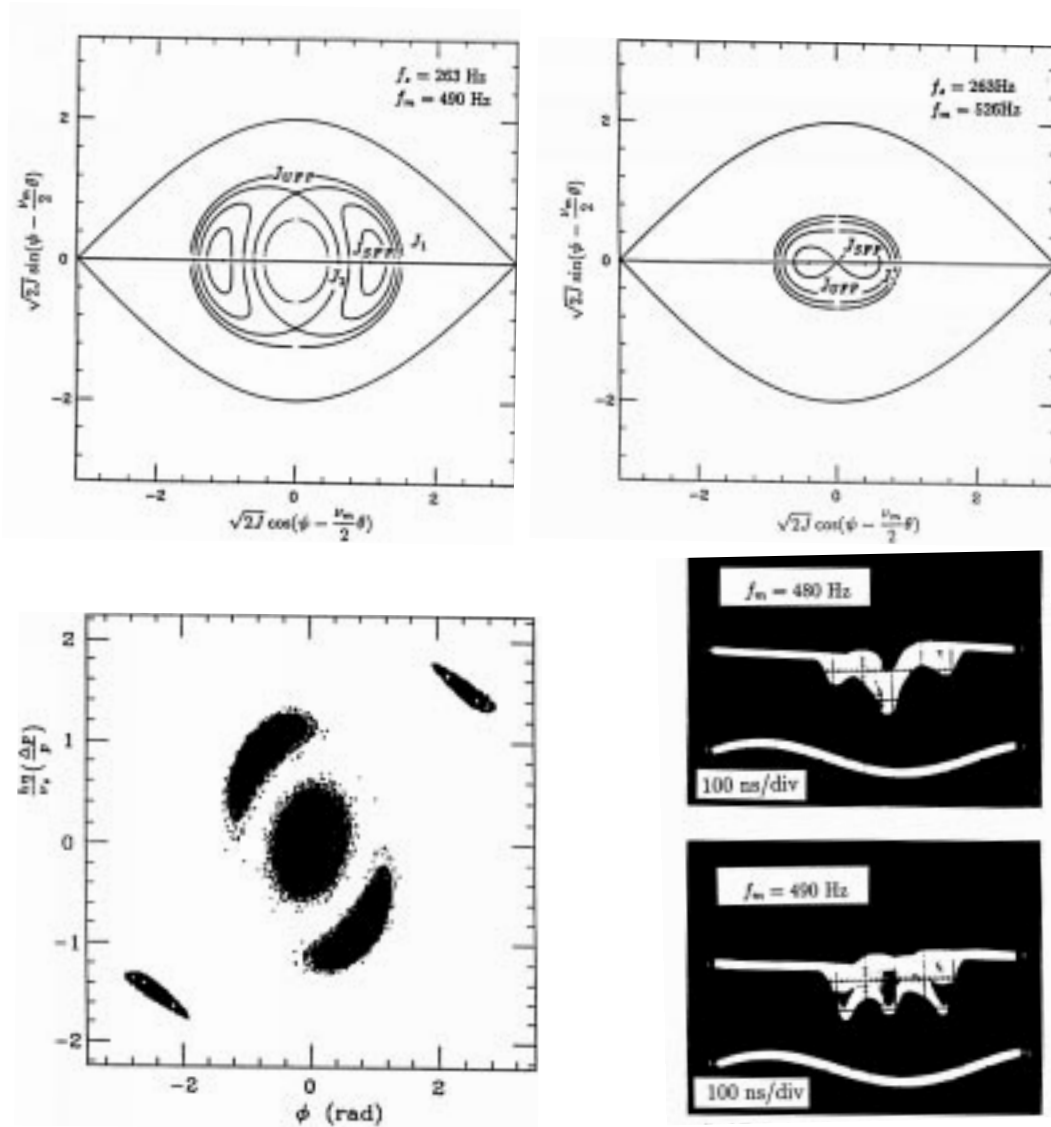


Figure 14: Top figures show separatrices and tori of the time-independent Hamiltonian with voltage modulation in multiparticle simulation for an experiment at IUCF. The modulation tune is below ν_2 with the formation of 3 islands on the left, while the modulation tune is above ν_2 with the formation of 2 islands on the right. The lower-left plot shows the final beam distribution when there are 3 islands, a damping rate of 2.5 s^{-1} has been assumed. The lower-right plot shows the longitudinal beam distribution from a BPM sum signal accumulated over many synchrotron periods. Note that the outer two beamlets rotate around the center beamlet at frequency equal to one-half the modulation frequency.

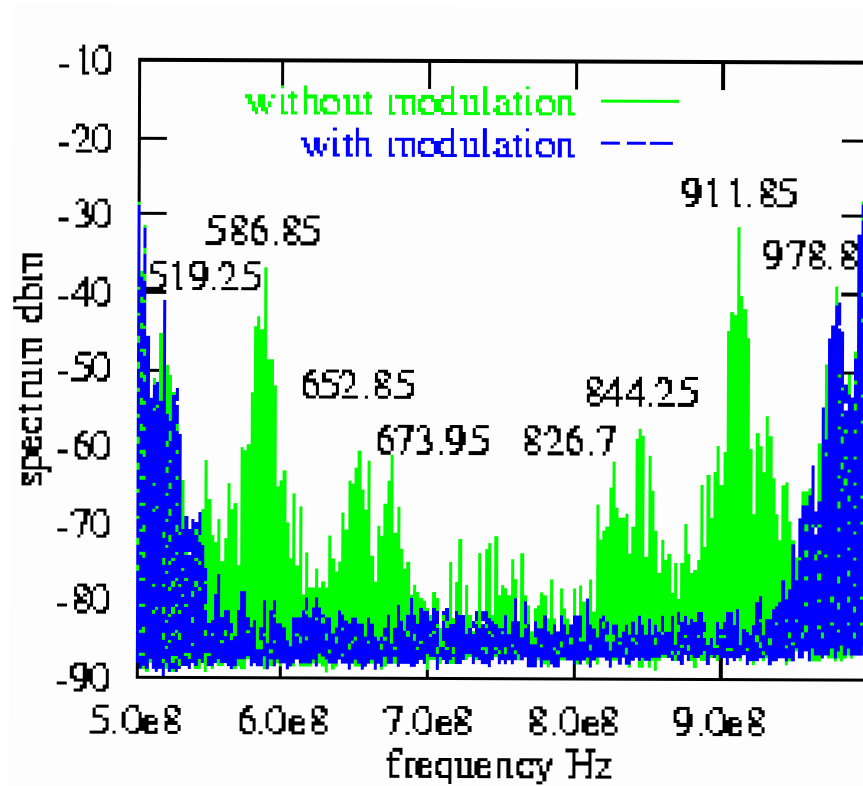


Figure 15: (color) Beam spectrum from BPM sum signal before and after applying rf voltage modulation. The modulation frequency was 50.155 kHz and the voltage modulation was 10%. The frequency span of the spectrum is 500 MHz.

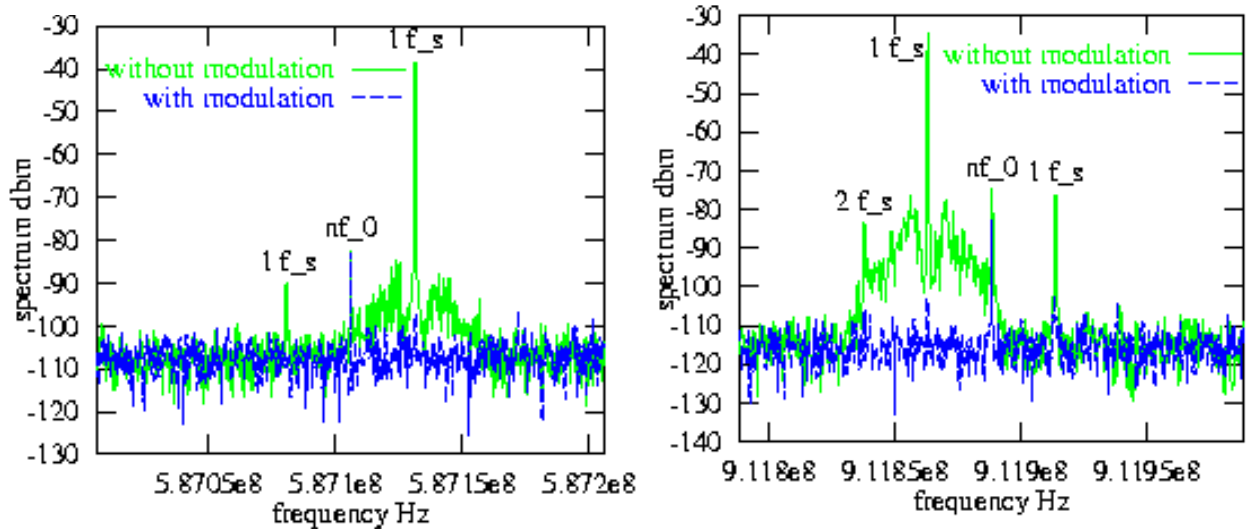


Figure 16: (color) Beam spectrum zoom in from Fig. 15. The revolution harmonic frequency of the left is 587.106 MHz and the right is 911.888 MHz. The frequency span of the spectrum is 200 kHz.

5 TRANSVERSE FOCUSING AND TRANSVERSE WAKE

Transverse focusing of the particle beam is necessary. If not the beam will diverge hitting the vacuum chamber and get lost. The alternating gradient focusing scheme employing F-quadrupoles and D-quadrupoles suggested by Courant and Synder [11] give very strong focusing of the beam in both the horizontal and vertical planes. For this reason, the transverse beam size can be made very small and so is the size of the vacuum chamber and the aperture of the magnets. In light sources, usually the Chasman-Green lattices are used. They consist of double achromats or triple achromats, which are strong focusing and give zero dispersion at both ends. Another merit of the achromats is that they can provide much smaller transverse emittances for the electron beam than the alternating gradient scheme of Courant and Synder.

Because quadrupoles can focus in only one transverse plane and defocus in the other, transverse oscillations develop in both transverse planes. These are called *betatron oscillations*, and the oscillation frequencies, $\omega_\beta/(2\pi)$, are called *betatron frequencies*, which are usually different in the two transverse plane. The number of betatron oscillations made in a revolution turn of the beam, $\nu_\beta = \omega_\beta/\omega_0$, is called the *betatron tune*. The equation of motion of a beam particle in, for example, the vertical plane, is given by

$$\frac{d^2y}{dn^2} + (2\pi\nu_\beta)^2 y = \frac{C_0^2 \langle F_1^\perp \rangle}{E_0}, \quad (5.1)$$

where the right side is the contribution due to the transverse electromagnetic wake $W_1(\tau)$. The transverse force averaged over the circumference of the ring, $\langle F_1^\perp \rangle$ acting on the test particle with time advance τ is defined as

$$\langle F_1^\perp(\tau) \rangle = \frac{e^2 D}{C_0} \int_{-\infty}^{\infty} d\tau' \rho(\tau') W_1(\tau' - \tau), \quad (5.2)$$

where ρ is the linear distribution of the beam which has a transverse offset D from the designed orbit. Correspondingly, one can define a *transverse impedance* $Z_1^\perp(\omega)$ in the frequency domain:

$$Z_1^\perp(\omega) = -i \int_{-\infty}^{\infty} e^{i\omega\tau} W_1(\tau) d\tau, \quad (5.3)$$

which has the dimension Ohms/m. In the definition, the $-i$ takes into account the fact that the force lags the displacement by $\frac{1}{2}\pi$.

There is a direct parallel between the transverse dynamics and the longitudinal dynamics, as is illustrated in the equations of motion in the longitudinal phase plane and the transverse phase plane. However, there is a big difference that the betatron tune $\nu_\beta \gg 1$ while the synchrotron tune $\nu_s \ll 1$.

6 TRANSVERSE COLLECTIVE INSTABILITIES

6.1 SEPARATION OF TRANSVERSE AND LONGITUDINAL MOTIONS

For bunched beam, longitudinal motion has to be included. Just as for synchrotron oscillations, it is more convenient to change from (y, p_y) to the circular coordinates (r_β, θ) in the transverse betatron phase

space. Following Eq. (2.1), we have

$$\begin{cases} y = r_\beta \cos \theta \\ p_y = r_\beta \sin \theta \end{cases}, \quad (6.1)$$

and Eq. (5.1) is transformed into

$$\begin{cases} \frac{dy}{ds} = -\frac{\omega_\beta}{v} p_y \\ \frac{dp_y}{ds} = \frac{\omega_\beta}{v} y - \frac{c}{E_0 \omega_\beta \beta} \langle F_1^\perp(\tau; s) \rangle \end{cases}, \quad (6.2)$$

where instead of turn number, the continuous variable s , denoting the distance along the designed orbit, has been used as the independent variable.

For time period much less than the synchrotron damping time, Hamiltonian theory can be used. The Hamiltonian for motions in both the longitudinal phase space and transverse phase space can be written as

$$H = H_\parallel + H_\perp, \quad (6.3)$$

where H_\parallel is the same Hamiltonian describing the longitudinal motion:

$$H_\parallel = -\frac{\eta}{2cE_0} (\Delta E)^2 + \frac{eh\omega_0^2 V_{\text{rf}} \cos \phi_s}{4\pi c} \tau^2 + V(\tau)|_{\text{wake}}, \quad (6.4)$$

while H_\perp is the additional term coming from the equations of motion in the transverse phase space as given by Eq. (6.2). We note that the transverse force $\langle F_1^\perp(\tau; s) \rangle$ in Eq. (6.2) depends on the longitudinal variable τ ; therefore

$$[H_\parallel, H_\perp] \neq 0. \quad (6.5)$$

We assume that the perturbation is small and synchro-betatron coupling is avoided. Then

$$[H_\parallel, H_\perp] \approx 0. \quad (6.6)$$

This implies that in the transverse phase space, the azimuthal modes $m_\perp = 1, 2, \dots$, and the radial modes $k_\perp = 1, 2, \dots$ are good eigen-modes. In fact, this is very reasonable because at small perturbation, the transverse azimuthal modes m_\perp correspond to frequencies $m_\perp \omega_\beta$ with separation ω_β . Since

$$\omega_\beta \gg \omega_0 \gg \omega_s, \quad (6.7)$$

the possibility for different transverse azimuthals to couple is remote. A direct result of Eq. (6.6) is the factorization of the bunch distribution Ψ in the combined longitudinal-transverse phase space; i.e.,

$$\Psi(r, \phi; r_\beta, \theta) = \psi(r, \phi) f(r_\beta, \theta), \quad (6.8)$$

where $\psi(r, \phi)$ is the distribution in the longitudinal phase space and $f(r_\beta, \theta)$ the distribution in the transverse phase space. Now decomposed ψ and f into the unperturbed parts and the perturbed parts:

$$\begin{aligned} \psi(r, \phi) &= \psi_0(r) + \psi_1(r, \phi), \\ f(r_\beta, \theta) &= f_0(r_\beta) + f_1(r_\beta, \theta). \end{aligned} \quad (6.9)$$

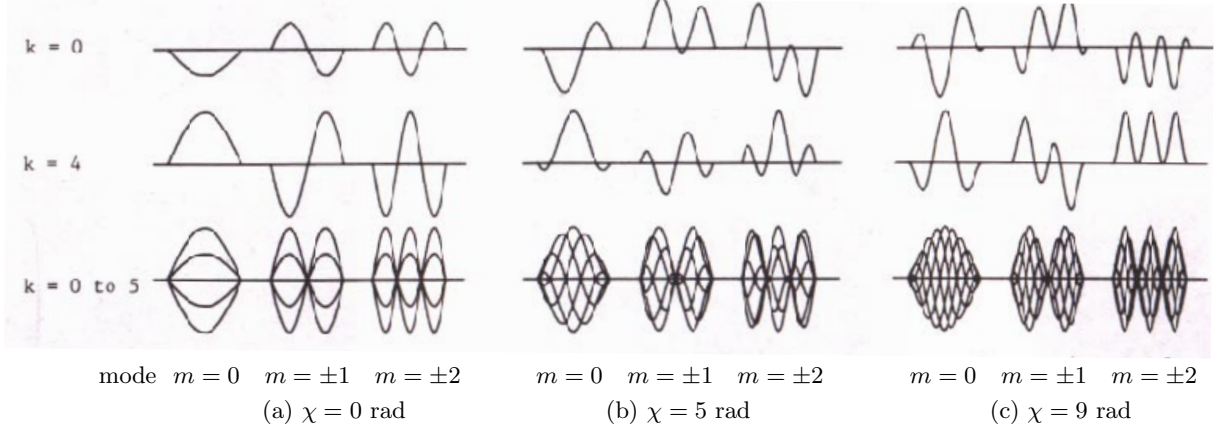


Figure 17: Head-tail modes of transverse oscillation. The plots show the contortions of a single bunch on separate revolutions, and with six revolution superimposed (denoted by k). Vertical axis is difference signal from position monitor, horizontal axis is time, and $\nu_\beta = 4.833$. The chromaticity phase are (a) $\chi = 0$ rad, (b) $\chi = 5$ rad, and (c) $\chi = 9$ rad.

When substituted into Eq. (6.8), there are four terms. The term $\psi_1 f_0$ implies only the longitudinal-mode excitations driven by the longitudinal impedance without any transverse excitations. This is what we have discussed in the previous sections and we do not want to include it again in the present discussion. The term $\psi_0 f_1$ describes the transverse excitations driven by the transverse impedance only. This term will be included in the $\psi_1 f_1$ term if we retain the azimuthal $m = 0$ longitudinal mode. For this reason, the bunch distribution Ψ in the combined longitudinal-transverse phase space contains only two terms

$$\Psi(r, \phi; r_\beta, \theta) = \psi_0(r) f_0(r_\beta) + \psi_1(r, \phi) f_1(r_\beta, \theta) e^{-i\Omega s/v} , \quad (6.10)$$

where we have separated out the collective angular frequency from $\psi_1 f_1$.

The next approximation is to consider only the rigid dipole mode in the transverse phase space; i.e., the bunch is displaced by an infinitesimal amount D from the center of the transverse phase space and executes betatron oscillations by revolving at frequency $\omega_\beta/(2\pi)$. Then we must have

$$f_1(r_\beta, \theta) = -D f'_0(r_\beta) e^{i\theta} . \quad (6.11)$$

This implies that all the modes that we are going to study are again synchrotron modes; but they are now sidebands of the betatron lines. Some of the transverse modes are shown in Fig. 17

Similar to Eq. (3.1) in the longitudinal dynamics, one can derive the growth rate of the imaginary part of the betatron tune shift or the shift of the synchrotron sideband:

$$\frac{1}{\tau_m} = \mathcal{I}m \Delta\omega_\beta = -\frac{eI_b c}{4\pi\nu_\beta E_0} \sum_{q=-\infty}^{+\infty} \mathcal{R}e Z_1^\perp(\omega_q) F_m(\omega_q) , \quad (6.12)$$

where $\omega_q = q\omega_0 + \omega_\beta + m\omega_s$. Notice that the coefficient of ω_β in the argument of $\mathcal{R}e Z_0^\perp$ is always unity, which reflects the fact that only the transverse rigid-dipole mode has been considered. The subscript ' m ' denotes

the azimuthal synchrotron modes adjacent to the betatron line. Unlike the case of pure longitudinal motion, the presence of ω_β in ω_q leaves the bunch spectrum without any symmetry between positive and negative frequencies. For this reason, we need to consider here synchrotron modes with both positive and negative frequencies; or m from $-\infty$ to ∞ . Writing the form factor F_m in terms of the power spectrum h_m of the m th azimuthal excitation illustrated in Fig. 5, we obtain from Eq. (6.12),

$$\frac{1}{\tau_m} = -\frac{1}{1+m} \frac{eI_b c}{4\pi\nu_\beta E_0} \frac{\sum_q \Re Z_1^\perp(\omega_q) h_m(\omega_q)}{B \sum_q h_m(\omega_q)}, \quad (6.13)$$

where $B = I_b/I_{pk}$ is the bunching factor. For a uniformly distributed bunch or the water-bag model, $B = f_0\tau_L$, where f_0 is the revolution frequency and τ_L the total length of the bunch. For the sake of convenience, one may normalize h_m in such a way that

$$B \sum_q h_m(\omega_q) = 1. \quad (6.14)$$

From the definition of the transverse impedance in Eq. (5.3), we see that $\Re Z_0^\perp(\omega)$ is antisymmetric in ω , being positive when $\omega > 0$ and negative when $\omega < 0$. Therefore, the formula for the growth in Eq. (6.13) shows that $\Re Z_0^\perp$ for negative frequency drives instability while $\Re Z_0^\perp$ for positive frequency stabilizes the beam.

6.2 CHROMATICITY FREQUENCY SHIFT

The betatron tune ν_β of a beam particle depends on its momentum offset δ through the chromaticity ξ , which is a property of the lattice of the accelerator and is defined as[‡]

$$\Delta\nu_\beta = \xi\delta, \quad (6.15)$$

Because the beam particle makes synchrotron oscillation, the betatron phase is continuously slipping. We would like to compute the phase slip for a particle that has a time advance τ relative to the synchronous particle. This is illustrated in Fig. 18.

The momentum offset in Eq. (6.15) can be eliminated using the equation of motion of the phase

$$\Delta\tau = -\eta T_0 \delta, \quad (6.16)$$

where η is the slip factor and $\Delta\tau$ is the change in time advance of the particle in a turn. The phase lag in a turn is then

$$\int 2\pi\Delta\nu_\beta = -2\pi\frac{\xi}{\eta} \int \frac{\Delta\tau}{T_0} = -\frac{\xi\omega_0}{\eta}\tau. \quad (6.17)$$

This means that the phase lag increases linearly along the bunch and is independent of the momentum offset. For a bunch of half length $\hat{\tau}$, the tail of the bunch, $\tau = -\hat{\tau}$, lags the head of the bunch, $\tau = +\hat{\tau}$, by the phase $2\hat{\tau}\omega_\xi$, where

$$\omega_\xi = \frac{\xi\omega_0}{\eta} \quad (6.18)$$

[‡]Sometimes, especially in Europe, the chromaticity ξ is also defined by $\Delta\nu_\beta = \xi\nu_\beta\delta$.

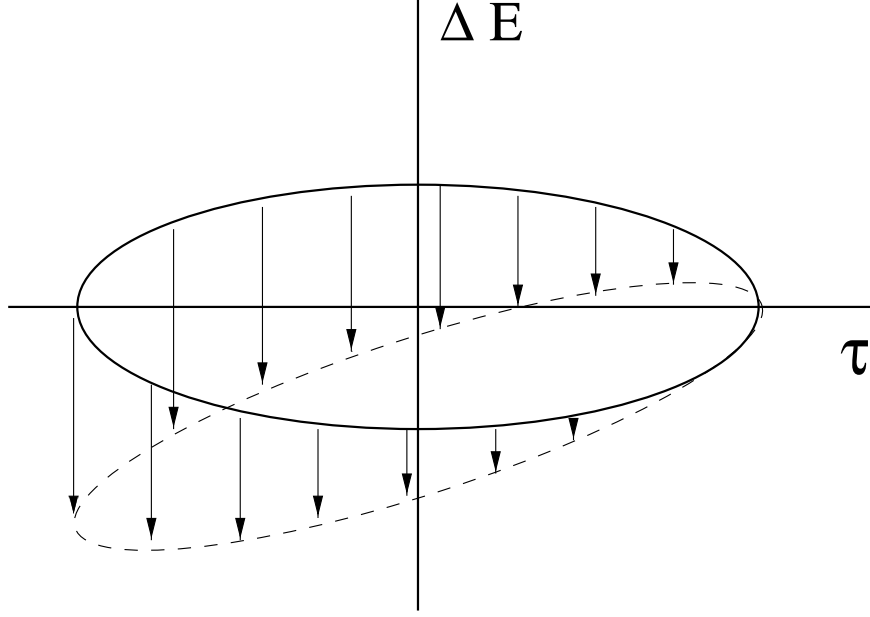


Figure 18: Schematic drawing showing the lagging of the betatron phase from the head (right) to the tail (left) of the bunch when the chromaticity ξ and slip factor η have the same signs.

is called the betatron angular frequency shift due to chromaticity. For this reason, ω_ξ should be subtracted from ω_q in the arguments of the power spectrum h_m and $\mathcal{R}e Z_1^\perp$ in Eq. (6.13). The total betatron tune shift from head to tail is represented by $\chi = \omega_\xi \tau_L$, where τ_L is the total length of the bunch from head to tail. The head-tail modes for various values of χ are shown in Fig. 17.

For positive chromaticity above transition, $\omega_\xi > 0$. The modes of excitation in Fig. 5 are therefore shifted to the right by the angular frequency ω_ξ . As shown in Fig. 19, mode $m = 0$ sees more impedance in positive frequency than negative frequency and is therefore stable. However, it is possible that mode $m = 1$, as in Fig. 19, samples more the highly negative $\mathcal{R}e Z_1^\perp$ at negative frequencies than positive $\mathcal{R}e Z_1^\perp$ at positive frequencies and becomes unstable.

If the transverse impedance is sufficiently smooth, it can be removed from the summation in Eq. (6.13). The growth rate for the $m = 0$ mode becomes

$$\frac{1}{\tau_0} = -\frac{eI_b c}{2\omega_\beta E_0 \tau_L} \mathcal{R}e Z_1^\perp(\omega_\xi). \quad (6.19)$$

The transverse impedance of the CERN PS had been measured in this way by recording the growth rates of a bunch at different chromaticities.

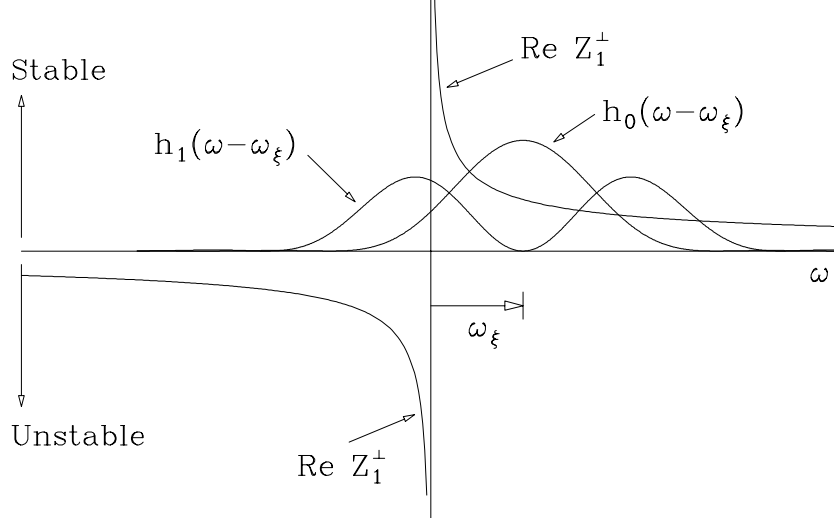


Figure 19: Positive chromaticity above transition shifts the all modes of excitation towards the positive frequency side by ω_ξ . Mode $m = 0$ becomes stable, but mode $m = 1$ may be unstable because it samples more negative $\mathcal{R}e Z_1^\perp$ than positive $\mathcal{R}e Z_1^\perp$.

7 TRANSVERSE COUPLED-BUNCH INSTABILITIES

7.1 RESISTIVE WALL

If there are M identical equally spaced bunches in the ring, there are $\mu = 0, \dots, M-1$ transverse coupled modes when the centers-of-mass of one bunch leads its predecessor by the betatron phase of $2\pi\mu/M$. The transverse growth rate for the μ -th coupled-bunch mode is exactly the same as the formula in Eq. (6.13) except for the replacement of ω_p by $\omega_q = (qM + \mu)\omega_0 + \omega_\beta + m\omega_s$; i.e.,

$$\frac{1}{\tau_{m\mu}} = -\frac{1}{1+m} \frac{eMI_b c}{4\pi\nu_\beta E_0} \frac{\sum_q \mathcal{R}e Z_1^\perp(\omega_q) h_m(\omega_q - \chi/\tau_L)}{B \sum_q h_m(\omega_q - \chi/\tau_L)}, \quad (7.1)$$

where the bunching factor $B = ML/C$ has been used and $\chi = \omega_\xi \tau_L$ is the chromaticity phase shift across the bunch of full length τ_L .

A most serious transverse coupled-bunch instability that occurs in nearly all storage rings is the one driven by the resistive wall. Since $\mathcal{R}e Z_1^\perp \propto \omega^{-1/2}$ and is positive (negative) when ω is positive (negative), a small negative frequency betatron line, which acts like a narrow resonance, can cause coupled-bunch instability. Take, for example, the Tevatron in the fixed target mode, where there are $M = 1113$ equally spaced bunches. The betatron tune is $\nu_\beta = 19.6$. The lowest negative betatron frequency line is at $(qM + \mu)\omega_0 + \omega_\beta = -0.4\omega_0$, for mode $\mu = 1093$ and $q = -1$. The closet damped betatron line ($q = 0$) is at $(1113 - 0.4)\omega_0$, but $\mathcal{R}e Z_1^\perp$ is only $-\sqrt{0.4/1112.6}$ the value at $-0.4\omega_0$. The next anti-damped betatron line ($q = -2$) is at $-1113.4\omega_0$, with $\mathcal{R}e Z_1^\perp$ equal to $\sqrt{0.4/1113.4}$ the value at $-0.4\omega_0$. This is illustrated in Fig. 20. Thus it is only the $-0.4\omega_0$ betatron line that dominates. From Eq. (7.1), the growth rate for this

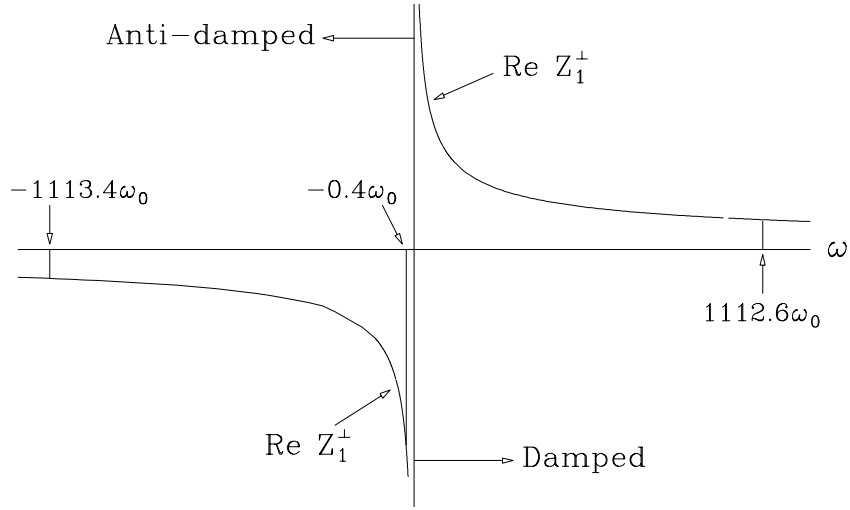


Figure 20: The $-0.4\omega_0$ betatron line in the Tevatron dominates over all other betatron lines for $\mu = 1093$ mode coupled-bunch instability driven by the resistive wall impedance.

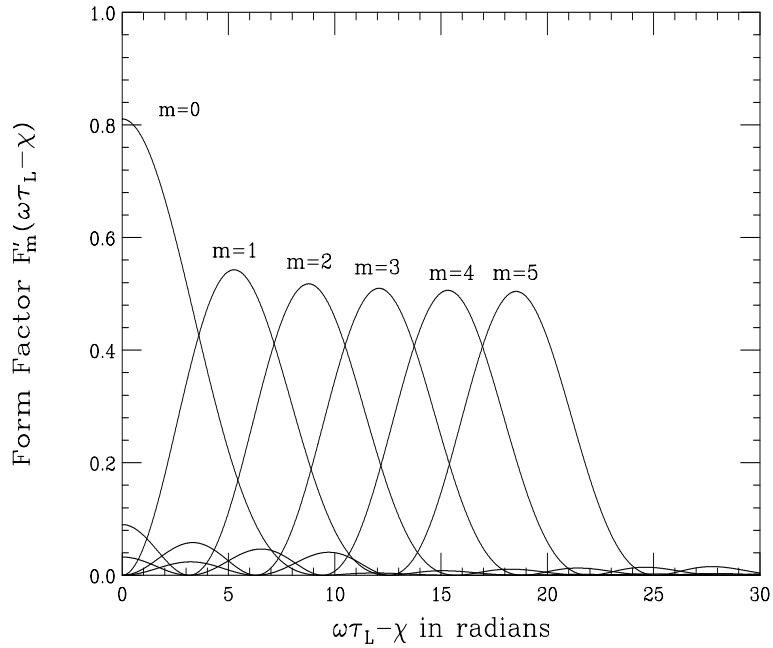


Figure 21: Plot of form factor $F'_m(\omega\tau_L - \chi)$ for modes $m = 0$ to 5. With the normalization in Eq. (6.14), these are exactly the power spectra h_m .

mode can therefore be simplified to

$$\frac{1}{\tau_{m\mu}} \approx -\frac{1}{1+m} \frac{eMI_b c}{4\pi\nu_\beta E_0} \mathcal{Re} Z_1^\perp(\omega_q) F'_m(\omega_q \tau_L - \chi), \quad (7.2)$$

where $\chi = \omega_\xi \tau_L$ and the form factor is

$$F'_m(\omega \tau_L) = \frac{2\pi h_m(\omega)}{\tau_L \int_{-\infty}^{\infty} h_m(\omega) d\omega}, \quad (7.3)$$

and is plotted in Fig. 21. For zero chromaticity, only the $m = 0$ mode can be unstable because the power spectra for all the $m \neq 0$ modes are nearly zero near zero frequency. Since the perturbing betatron line is at extremely low frequency, we can evaluate the form factor at zero frequency. For the sinusoidal modes, we get $F'(0) = 8/\pi^2 = 0.811$. One method to make this mode less unstable or even stable is by introducing positive chromaticity when the machine is above transition. For the Tevatron, $\eta = 0.0028$, total bunch length $\tau_L = 5$ ns, revolution frequency $f_0 = 47.7$ kHz, a chromaticity of $\xi = +10$ will shift the spectra by the amount $\omega_\xi \tau_L = 2\pi f_0 \xi \tau_L / \eta = 5.4$. The form factor and thus the growth rate is reduced by more than 4 times. However, from Figs. 5 and 19, we see that the spectra are shifted by $\omega_\xi \tau_L / \pi = 1.7$ and the $m = 1$ mode becomes unstable. Another method for damping is to introduce a betatron angular frequency spread using octapoles, with the spread larger than the growth rate.

A third method is to employ a damper. Let us derive the displacements of consecutive bunches at a BPM. Suppose the first bunch is at the BPM with betatron phase $\phi_{\beta 0} = 0$; its displacement registered at the BPM is proportional to $\cos \phi_{\beta 0} = 1$. At that moment, the next bunch has phase $2\pi\bar{\mu}/M$ in advance, where $\bar{\mu} = qM + \mu = -20$. When this bunch arrives at the BPM, the time elapsed is T_0/M and the change in betatron phase is $\omega_\beta T_0/M = 2\pi\nu_\beta/M$. The total betatron phase on arrival at the BPM is therefore $\phi_{\beta 1} = 2\pi\bar{\mu}/M + 2\pi\nu_\beta/M = 2\pi(\bar{\mu} - \nu_\beta)/M = (-0.4)2\pi/M$, and the displacement registered is $\cos \phi_{\beta 1}$. When the n th consecutive bunch arrives at the BPM, its phase will be $\phi_{\beta n} = n(-0.4)2\pi/M$. This is illustrated in Fig. 22 when the BPM is registering every 20th bunch. What we see at the BPM is a wave of frequency -0.4 harmonic or about 19.1 kHz. Because we know that the bunches follow the pattern of such a slow wave, we only require a very narrow-band feedback system will damp the instability. Usually the adjacent modes $\mu = 1092, 1091, \dots$ will also be unstable at the $-1.4\omega_0, -2.4\omega_0, \dots$ betatron line; but the growth rates will be smaller.

7.2 NARROW RESONANCES

The narrow higher-order transverse resonant modes of the rf cavities will also drive transverse coupled-bunch instabilities. The growths rate are described by the general growth formula of Eq. (7.1). When the resonance is narrow enough, only the betatron lines closest to the resonant frequency $\omega_r/(2\pi)$ contribute in the summation. The growth rate is therefore given by Eq. (7.2), where two betatron lines are included.

$$\frac{1}{\tau_{m\mu}} \approx -\frac{1}{1+m} \frac{eMI_b c}{4\pi\nu_\beta E_0} [\mathcal{Re} Z_1^\perp(\omega_q) F'_m(\omega_q \tau_L - \chi) - \mathcal{Re} Z_1^\perp(\omega_{q'}) F'_m(\omega_{q'} \tau_L - \chi)], \quad (7.4)$$

where q and q' satisfy

$$\begin{cases} -\omega_r \approx \omega_q = (qM + \mu + \nu_\beta + m\nu_s)\omega_0 \\ \omega_r \approx \omega_{q'} = (q'M + \mu + \nu_\beta + m\nu_s)\omega_0. \end{cases} \quad (7.5)$$

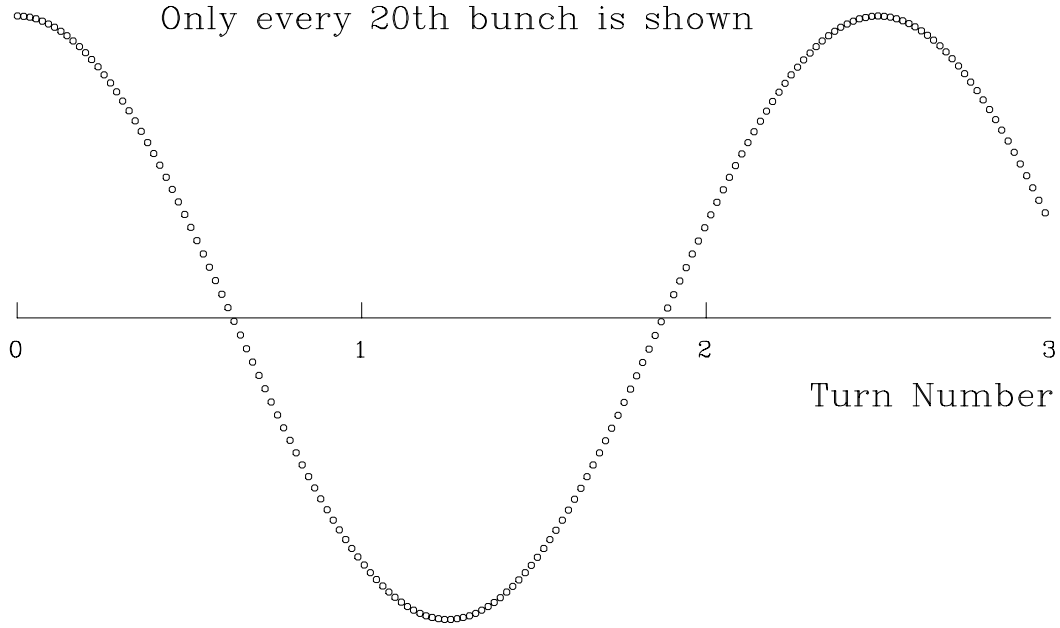


Figure 22: Difference signal at a BPM displaying the displacement of every 20th bunch, when the $\mu = 1093$ mode of transverse coupled-bunch is excited by the resistive wall impedance.

Similar to the situation of longitudinal coupled-bunch instabilities, mode $\mu = 0$ and mode $\mu = M/2$ if M is even receive contributions from both the positive-frequency side and negative-frequency side. In the language of only positive frequencies, there are the upper and lower betatron side-bands flanking each revolution harmonic line. The lower side-band originates from negative frequency and is therefore anti-damped. For these two modes, both the upper and lower side-bands correspond to the same coupled-bunch mode. If the resonant frequency of the resonance leans more towards the lower sideband, there will be a growth. If the resonant frequency leans more towards the upper side band, there will be damping. This is the Robinson's stability analog in the transverse phase plane. However, sometimes it is not so easy to identify which is the lower sideband and which is the upper sideband. This is because the residual betatron tune $[\nu_\beta]$ or the noninteger part of the betatron tune can assume any value between 0 and 1. If $[\nu_\beta] > 0.5$, the upper betatron sideband of a harmonic will have a higher frequency than the lower betatron sideband of the next harmonic.

There is one important difference between transverse coupled-bunch instabilities driven by the resistive-wall impedance and by the higher-order resonant modes. The former is at very low frequency and therefore the form factor F_1 is close to 1 when the chromaticity is zero. The latter, however, is at the high frequency of the resonances. The form factor usually assumes a much smaller value unless than bunch is very short and we sometimes refer this to “damping” from the spread of the bunch.

This instability can be observed easily in the frequency domain at the lower betatron sidebands flanking the harmonic lines. If a particular lower betatron sideband grows strongly, we subtract the betatron tune ν_β (not $[\nu_\beta]$) to find out which harmonic line it is associated with. Then from Eq. (7.5), we can determine

which coupled-bunch mode μ it is. To damp this transverse coupled-bunch instability, one can identify the offending resonant modes in the cavities and damp them passively using an antenna. A tune spread due to the slip factor η or from an octupole can also contribute to the damping. When the above are not efficient enough, a transverse bunch-to-bunch damper will be required. Unlike the situation of the resistive wall, here the damper must be of wide-band.

8 HEAD-TAIL INSTABILITIES

Let us now consider the short-range field of the transverse impedance; i.e., $Z_1^\perp(\omega)$ when ω is large. This is equivalent to replacing the discrete line spectrum by a continuous spectrum. Since $\mathcal{R}e Z_\perp(\omega)$ is antisymmetric, the summation in Eq. (6.13) when transformed into an integration will vanish identically at zero chromaticity. There can only be instability when the chromaticity is nonzero. The growth rate for the m -th azimuthal mode is therefore

$$\frac{1}{\tau_m} = -\frac{1}{1+m} \frac{\pi e c I_b}{E_0 \omega_\beta \omega_0^2 \tau_L^2} \int_{-\infty}^{\infty} d\omega \mathcal{R}e Z_1^\perp(\omega) h_m(\omega - \omega_\xi) . \quad (8.1)$$

Note that the factor of M , the number of bunches, in the numerator and denominator cancel. This is to be expected because the growth mechanism is driven by the short-range wake field and the instability is therefore a single-bunch effect. This explains why the growth rate τ_m^{-1} does not contain the subscript μ describing phase relationship of consecutive bunches.

Let us demonstrate this by using only the resistive wall impedance. The resistive wall impedance of the vacuum chamber is

$$Z_1^\perp(\omega) = [1 - i \operatorname{sgn}(\omega)] \frac{C_0 c}{\pi \omega b^3 \sigma_c \delta_{\text{skin}}} , \quad (8.2)$$

where b is the beam-pipe radius, σ_c the wall conductivity, and δ_{skin} the wall skin depth. When this is substituted into Eq. (6.13), the result of the integration over ω gives [12]

$$\frac{1}{\tau_m} = -\frac{1}{1+m} \frac{e I_b c}{4 \nu_\beta E} \left(\frac{2}{\omega_0 \tau_L} \right)^{1/2} |Z_1^\perp(\omega_0)| F_m(\chi) , \quad (8.3)$$

where $|Z_1^\perp(\omega_0)|$ is the magnitude of the resistive wall impedance at the revolution frequency. The form factor is given by

$$F_m(\chi) = \sqrt{\frac{2}{\pi}} \int_0^\infty \frac{dy}{\sqrt{y}} [h_m(y - y_\xi) - h_m(y + y_\xi)] , \quad (8.4)$$

where h_m are power spectra of the m -th excitation mode in Fig. 5 written as functions of $y = \omega \tau_L / \pi$ and $y_\xi = \chi / \pi = \xi \omega_0 \tau_L / (\pi \eta)$. The first term in the integrand comes from contributions by positive frequencies while the second term by negative frequencies. The form factors for $m = 0$ to 5 are plotted in Fig. 23.

This single-bunch instability will occur in nearly all machines. The $m = 0$ mode is the rigid-bunch mode when the whole bunch oscillates transversely as a rigid unit. For the $m = 1$ mode, the head of the bunch moves transversely in one direction while the tail moves transversely in the opposite direction with the center-of-mass stationary, and is called the dipole head-tail mode. This is the head-tail instability first analyzed by Pellegrini and Sands [13, 14].

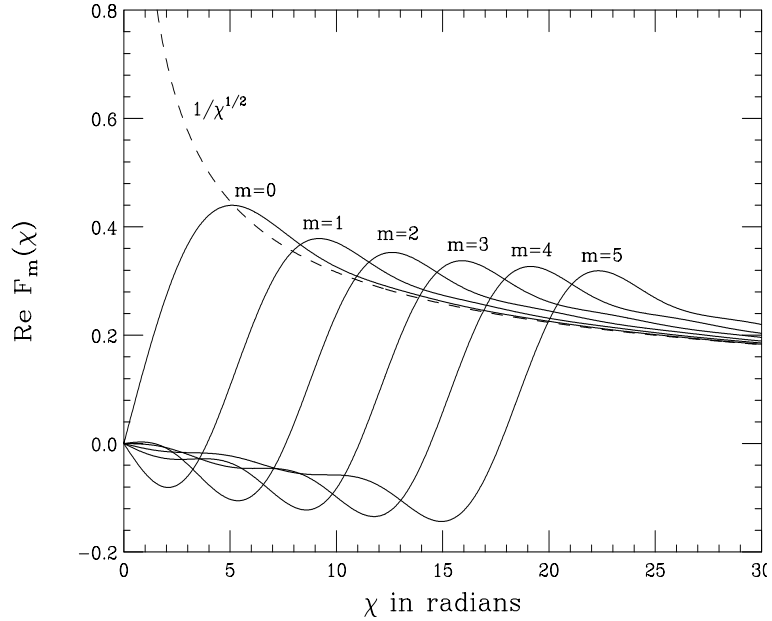


Figure 23: Form factor $F_m(\chi)$ for head-tail instability for modes $m = 0$ to 5.

For small chromaticity $\xi \lesssim 4$, $\chi \lesssim 2.3$ the integrand in Eq. (8.4) can be expanded and the growth rate becomes proportional to chromaticity. The form factor has been computed listed in Table I, where negative sign implies damping. We see from Table I that mode $m = 0$ is stable for positive chromaticity. This is expected because the excitation spectrum for this mode has been pushed towards the positive-frequency side. All other modes ($m > 0$) should be unstable because their spectra see relatively more negative $\Re Z_1^\perp$. Looking into the form factors in Fig. 23, however, the growth rate for $m = 4$ is tiny and mode $m = 2$ is even stable. This can be clarified by looking closely into the excitation spectra in Fig. 5. We find that while mode $m = 0$ has a large maximum at zero frequency, all the other higher even m modes also have small maxima at zero frequency. As these even m spectra are pushed to the right, these small central maxima see more impedance from positive frequency than negative frequency. Since these small central maxima are near zero frequency where $|\Re Z_1^\perp|$ is large, their effect may cancel out the opposite effect from the larger maxima which interact with the impedance at much higher frequency where $|\Re Z_1^\perp|$ is smaller. This anomalous effect does not exist in the Legendre modes or the Hermite modes, because the corresponding power spectra vanish at zero frequency when $m > 0$.

Although the head-tail instabilities can be damped by the incoherent spread in betatron frequency, it is advisable to run the machine at a negative chromaticity above transition. In this case, all the higher modes with $m \neq 0$ will be stable, and the unstable $m = 0$ mode can be damped with a damper.

Head-tail modes of oscillations can be excited shifting the chromaticity to the unstable direction and observed using a wide-band pickup. These modes were first observed in the CERN PS Booster [15] and

Table I: Linearized form factor of transverse head-tail modes driven by the resistive wall impedance when $\chi \lesssim 2.3$.

Mode	Form Factor
m	F_m
0	-0.1495χ
1	$+0.0600 \chi$
2	-0.0053χ
3	$+0.0191 \chi$
4	$+0.0003 \chi$
5	$+0.0098 \chi$

depicted in Fig. 24. They have also been measured in the Fermilab Rings.

The head-tail instability comes about because of nonzero chromaticity or the betatron tune is a function of energy spread. There is also such an analog in the longitudinal phase space, where the slip factor η is energy-spread dependent. The longitudinal beam distribution then picks up a head-tail phase and instability may arise [16]. In fact, longitudinal head-tail instability had been observed at the CERN SPS [17] and it was also seen at the Fermilab Tevatron.

9 STRONG HEAD-TAIL INSTABILITY

In the growth rate formula of Eq. (6.13), we consider each individual mode separately. As the beam intensity increases, the shift of each azimuthal mode becomes so big that two adjacent modes overlap each other. The azimuthal mode number is no longer a good eigen-number, and we can no longer represent the perturbation distribution ψ_1 as a single azimuthal mode; instead it should be a linear combination of all azimuthal modes. This phenomenon has been referred to as *strong head-tail* or *transverse turbulence* in parallel with the longitudinal mode-mixing or longitudinal microwave instability studied earlier.

Let us consider transverse instability driven by a broad-band impedance. This implies a single bunch mechanism. Also we set the chromaticity to zero. For the m -th azimuthal mode and k -th radial mode, Eq. (6.13) or (7.1) becomes

$$(\Omega - m\omega_s)\delta_{mm'}\delta_{kk'} = M_{mm'kk'} \quad (9.1)$$

where, with the aid of Eq. (6.13), the matrix M is defined as

$$M_{mm'kk'} = -\frac{ieI_b c}{2\omega\beta E_0\tau_L} \frac{\int d\omega Z_1^\perp(\omega)\tilde{\lambda}_{m'k'}(\omega)\tilde{\lambda}_{mk}^*(\omega)}{\int d\omega\tilde{\lambda}_{mk}(\omega)\tilde{\lambda}_{mk}^*(\omega)}. \quad (9.2)$$

The summations have been converted to integrations because the impedance is so broad-band that there is no need to distinguish the individual betatron lines. A further simplification is to keep only the first most easily excited radial modes. Then, the problem becomes coupling in the azimuthal modes.

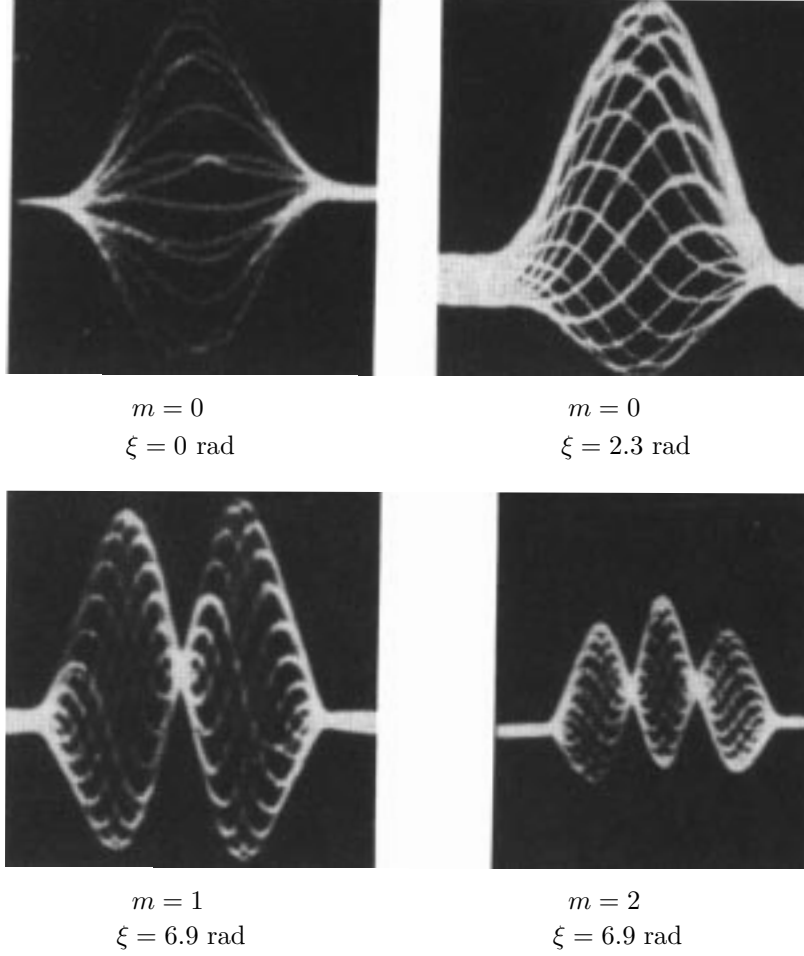


Figure 24: A single bunch in the CERN PS Booster seen on about 20 consecutive revolutions with a wide-band pickup (bandwidth ~ 150 MHz). Vertical axis: difference pickup signal. Horizontal axis: time (50 ns per division). The azimuthal mode number and chromaticity in each plot are as labeled.

Since $\text{Re } Z_1^\perp(\omega)$ is odd in ω and $\text{Im } Z_1^\perp(\omega)$ is even in ω , only $\text{Im } Z_1^\perp(\omega)$ will contribute to the diagonal terms of the matrix M giving only real frequency shifts which will not lead to instability. As the beam current becomes larger, two modes will collide and merge together, resulting in two complex eigen-frequencies, one is the complex conjugate of the other, thus introducing instability. Therefore, coupling should originate from the off-diagonal elements closest to the diagonal. It can be easily shown that the m -th mode of excitation $\tilde{\lambda}_m(\omega)$ is even in ω when m is even, and odd in ω when m is odd. Thus, it is $\text{Re } Z_1^\perp(\omega)$ that gives the coupling.

The eigen-angular-frequencies are solved by

$$\det[(\Omega - \omega_\beta - m\omega_s)I - M] = 0 . \quad (9.3)$$

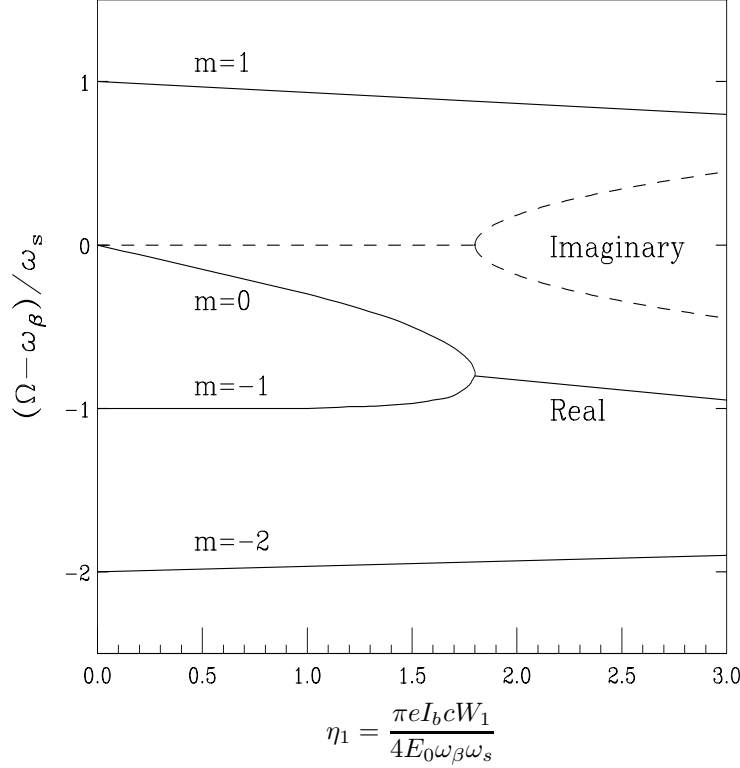


Figure 25: Transverse mode frequencies $(\Omega - \omega_\beta) / \omega_s$ versus the current intensity parameter η_1 for an air-bag bunch distribution perturbed by a constant wake potential W_1 . The instability occurs at $\eta_1 \approx 1.8$, when the $m = 0$ and $m = 1$ modes collide. The dashed curves are the imaginary part of the mode frequencies or growth/damping rate for the two colliding modes.

As an example, an airbag model is perturbed by the impedance

$$Z_1^\perp(\omega) = \frac{W_1}{\omega + i\epsilon} = \wp\left(\frac{W_1}{\omega}\right) - i\pi W_1 \delta(\omega), \quad (9.4)$$

which corresponds to a constant wake function W_1 . The infinite matrix is truncated and the eigenvalues solved numerically. The solution is shown in Fig. 25 [18]. This impedance corresponds to a real part that falls off as frequency increases. The imaginary part is a δ -function at zero frequency, and therefore interacts with the $m = 0$ mode only. This explains why all other modes remain almost unshifted with the exception of $m = 0$. The downward frequency shift of the $m = 0$ mode as the beam intensity increases from zero is a general behavior for short bunches. The transverse wake force produced by an off-axis beam has the polarity that deflects the beam further away from the pipe axis. This force acts as a defocusing force for the rigid beam mode, and therefore the frequency shifts downward. Such a down shift of the betatron frequency is routinely observed in electron accelerators and serves as an important tool of probing the impedance. Eventually the $m = 0$ shifts downwards and meets with the $m = -1$ mode, thus exciting an instability. The threshold is at

$$\eta_1 = \frac{\pi e I_b c W_1}{4 E_0 \omega_\beta \omega_s} \approx 1.8, \quad (9.5)$$

and is bunch-length independent. We can also obtain an approximate threshold from Eqs. (9.1) and (9.2) by equating the frequency shift to ω_s , and get

$$\frac{eI_b c Z_1^\perp|_{\text{eff}}}{2E_0 \omega_\beta \omega_s \tau_L} \approx 1, \quad (9.6)$$

where

$$Z_1^\perp|_{\text{eff}} = \frac{\int d\omega Z_1^\perp(\omega) h_m(\omega)}{\int d\omega h_m(\omega)} \quad (9.7)$$

is called the effective transverse impedance for mode m . Comparing Eqs. (9.5) and (9.6), we find the two thresholds are almost the same except for the bunch-length dependency, which we think should be understood as follows. Since the imaginary part of the impedance in Eq. (9.4) is a δ -function at zero frequency which interacts only with the $m = 0$ mode. As the bunch length becomes shorter, the spectrum spreads out wider, so that the spectrum at zero frequency becomes smaller. In fact, from the power spectrum and its normalization in Eq. (6.14), it is clear that $Z_1^\perp|_{\text{eff}} \propto \tau_L$, thus explaining why η_1 in Eq. (9.5) is bunch-length independent.

Now consider the situation when the impedance is a broad-band resonance. For a very short bunch, the $m = 0$ mode extends to very high frequencies and will cover part of the high-frequency capacitive part of the resonance. Thus the effective impedance $Z_1^\perp|_{\text{eff}}$ can become small due to the cancellation of the inductive and capacitive parts. At the same time, the peak of $\text{Re} Z_1^\perp$ is far from the peak of the $m = 1$ mode, thus making the coupling between the $m = 0$ and $m = 1$ mode very weak. Since the frequency shift is small and the coupling is weak, it will take a much higher beam current for the $m = 0$ mode to meet with the $m = 1$ mode, thus pushing up the threshold current. For a long bunch, the $m = 0$ mode has a small frequency spread. If it stays inside the inductive region where $\text{Im} Z_1^\perp$ is almost constant, $Z_1^\perp|_{\text{eff}}$ will be almost constant and the threshold current increase linearly with the bunch length. When the bunch is very long, the $m = \pm 1$ and even $m = \pm 2$ and $m = \pm 3$ modes may stay inside the constant inductive region of the impedance. This implies that the higher azimuthal modes also interact strongly with the impedance and these mode will have large shifts so that the threshold can become much smaller. Several collisions may occur around a small beam-current interval and the bunch can become very unstable suddenly.

The transverse mode-coupling instability was first observed at PETRA and later also at PEP and LEP. The strong head-tail instability is one of the cleanest instabilities to observe in electron storage rings [19]. In particular, one may measure the threshold beam intensity when the beam becomes unstable transversely. Another approach is to measure the betatron frequency as the beam intensity is varied. From the shift of the betatron frequency per unit intensity increase, the transverse wake can be inferred. The transverse motion of the bunch across its length can also be observed easily using a streak camera.

In the longitudinal mode-mixing instability, the bunch lengthens as the beam becomes unstable essentially without losing beam particles. This does not happen in the transverse case. The instability is devastating; as soon as the threshold is reached, the bunch disappears. However, so far no strong head-tail instabilities have ever been observed in hadron machines.

Radiation damping is too slow to damp the strong head-tail instability. A damper significantly faster

than ω_s is required. As shown in Fig. 25, it is mode $m = 0$ that is shifted downward to collide with mode $m = -1$ so as to start the instability. But mode $m = 0$ is the pure rigid dipole betatron oscillation with synchrotron motion. Therefore if we can introduce a positive coherent betatron tune shift, it will slow this mode from coming down and therefore push the threshold to a higher value. A conventional feedback system is resistive; i.e., the kicker is located at an odd multiple of 90° from the pickup. Here, a reactive feedback system is preferred [20]. The kicker is located at an even multiple of 90° from the pickup. In a two-particle model, where the bunch is represented by two macroparticles, the equations of motion are, in the first half of the synchrotron period,

$$\begin{aligned}\frac{d^2 y_1}{dn^2} + (2\pi\nu_\beta)^2 y_1 &= \sigma(y_1 + y_2) , \\ \frac{d^2 y_2}{dn^2} + (2\pi\nu_\beta)^2 y_2 &= \sigma(y_1 + y_2) + \alpha y_1 ,\end{aligned}\tag{9.8}$$

where y_1 and y_2 are, respectively, the transverse displacements of the head and tail macroparticles, σ is the gain of the reactive feed back, and α represents the effect of the transverse wake from head to tail. Notice that the reactive feedback acts on the center of the bunch and is in phase with the particle displacements. It therefore modifies ν_β by introducing a tuneshift. The instability threshold can then be raised by properly choosing the feedback strength σ . In low-energy hadron machines, the space-charge tune shift constitutes a natural reactive feedback system which tends to shift the $m = 0$ mode upwards.

This instability can also be damped by BNS damping [21], which delivers a betatron tune spread from the head of the bunch to the tail. This can be achieved by tilting the longitudinal phase space distribution of the bunch so that the tail has a lower energy relative to the head through chromaticity. Another method to implement BNS damping is to introduce a radio-frequency quadrupole magnet system, so that particle along the bunch will see a graduate shift in betatron tune.

References

- [1] C. Bernardini, *et al*, Phys. Rev. Lett. **10**, 407 (1963).
- [2] E. Keil and W. Schnell, CERN Report TH-RF/69-48 (1969); V.K. Neil and A.M. Sessler, Rev. Sci. Instr. **36**, 429 (1965); D. Boussard, CERN Report Lab II/RF/Int./75-2 (1975).
- [3] S. Krinsky and J.M. Wang, Particle Accelerators **17**, 109 (1985).
- [4] A.W. Chao and J. Gareyte, Part. Accel. **25**, 229 (1990).
- [5] P. Krejcik, K. Bane, P. Corredoura, F.J. Decker, J. Judkins, T. Limberg, M. Minty, R.H. Siemann, and F. Pedersen, *High Intensity Bunch Length Instabilities in the SLC Damping Ring*, Proc. 1993 Particle Accelerator Conference and International Conference on High-Energy Accelerators, Washington, DC, May 17-20, 1993, p.3240.
- [6] P.B. Robinson, *Stability of Beam in Radiofrequency System*, Cambridge Electron Accel. Report CEAL-1010, 1964.
- [7] A. Hofmann and S. Myers, *Beam Dynamics in a Double RF System*, Proc. 11th Int. Conf. High Energy Accel., Geneva, 1980.

- [8] A. Mosnier, *Cures of Coupled Bunch Instabilities*, PAC'99, Paper FRBR2.
- [9] D. Li, M. Ball, B. Brabson, J. Budnick, D.D. Caussyn, A.W. Chao, V. Derenchuk, S. Dutt, G. East, M. Ellison, D. Friesel, B. Hamilton, H. Huang, W.P. Jones, S.Y. Lee, J.Y. Liu, M.G. Minty, K.Y. Ng, X. Pei, A. Riabko, T. Sloan, M. Syphers, Y. Wang, Y. Yan, and P.L. Zhang, '*Effects of Rf Voltage Modulation on Particle Motion*', Nucl. Inst. Meth. **A364**, 205 (1995).
- [10] M.H. Wang, Peace Chang, P.J. Chou, K.T. Hsu, C.C. Kuo, J.C. Lee, and W.K. Lau, *Experiment of RF Voltage Modulation at at SRRC*, PAC'99, Paper THA106.
- [11] E.D. Courant and H.S. Snyder, *Theory of the Alternating-Gradient Synchrotron*, Annals of Physics **3**, 1 (1958).
- [12] F.J. Sacherer, *Theoretical Aspects of the Behaviour of Beams in Accelerators and Storage Rings*, Proc. First Course of Int. School of Part. Accel., Erice, Nov. 10-22, 1976, p.198.
- [13] C. Pellegrini, Nuovo Cimento **64**, 447 (1969).
- [14] M. Sands, SLAC-TM-69-8 (1969).
- [15] K. Hübner, P. Strolin, V. Vaccaro, and B. Zotter, *Concerning the Stability of the ISR Beam Against Coherent Dipole Oscillations*, CERN/ISR-RF-TH/70-2 (1970).
- [16] B. Chen, *The Longitudinal Collective Instabilities of Nonlinear Hamiltonian Systems in a Circular Accelerator*, Thesis, U. of Texas at Austin, May, 1995.
- [17] D. Boussard and T. Linnekar, Proc. 2nd EPAC, Nice, 1990, ed. Marin and Mandrillon, p.1460.
- [18] A.W. Chao, *Physics of Collective Beam Instabilities in High Energy Accelerators*, John Wiley & Sons, 1993, p. 251.
- [19] R. Kohaupt, IEEE Trans. Nucl. Sci. **NS-26**, 3480 (1979); D. Rice, et al., IEEE Trans. Nucl. Sci. **NS-28**, 2446 (1981); PEP Group, Pro. 12th Int. Conf. High Energy Accel. Fermilab, 1983, p.209.
- [20] R. Ruth, CERN Report LEP-TH/83-22 (1983); S. Myers, Proc. IEEE Part. Accel. Conf., Washington, 1987, p.503; B. Zotter, IEEE Trans. Nucl. Sci. **NS-32**, 2191 (1985); S. Myers, CERN Report LEP -523 (1984).
- [21] V. Balakin, A. Novokhatsky, and V. Smirnov, Proc. 12th Int. Conf. High Energy Accel., Fermilab, 1983, p.11.